

## Chapter 1: Introduction

### 1.1 Overview

Restoring lost and degraded wetlands is essential to ensure the health of our watersheds. Over the past 200 years, historic tidal wetlands have been destroyed at an alarming rate (*EPA factsheet*, 2001). Such reduction of tidal wetlands hamper various functions like water quality protection, habitat for fish and other wildlife, and flood protection. Unless reserving the tide of wetland loss, the quality of waters will continue to be threatened and part of natural heritage will be lost.

Restoration is the return of a degraded wetland or former wetland to its preexisting, naturally functioning condition, or a condition as close to that as possible (*EPA factsheet*, 2001). It is a complex process that requires expertise, resource and commitments from many different stakeholders. The timing of the restoration activities will be important not only to avoid disturbing wildlife species but also to ensure that earlier phases of the restoration have been successful before altering other habitat. It will be necessary to carefully monitor conditions as the restoration proceeds, and adapt the restoration plans to ensure overall project goals are achieved. Restoration projects require planning, implementation, monitoring and management, using a team with expertise in ecology, hydrology, engineering and environmental planning. Shallow estuaries are extremely dynamic regions where fluid motions are associated with both surface waves and current. Its restoration requires a number of factors to be taken into consideration.

The proper design as well as construction and maintenance of restoration work needs the exact knowledge of hydrodynamics. There are several physical conditions that will affect the feasibility of restoring tidal marshes: presence of channels, availability of material for levees, pond subsidence, potential for flooding, and infrastructure impediments (bridges, harbours,

lock gates, etc.). The insight of spatial and temporal variability of flow velocity is the major factor controlling the morphology of the system. The erosion and sedimentation processes of tidal marsh have an important effect on the proper functioning of estuary. The use of numerical models in the restoration of a nature reserve has a great importance in terms of development and evaluation of ever changing tidal system. Therefore, the hydrodynamic investigation is chosen to be a major part of a nature reserve restoration project.

## **1.2 Objective of the study**

The main objective of this thesis is to study the hydrodynamic processes in the nature reserve at 'De IJzermonding'. A two dimensional numerical model, TELEMAC-2D is chosen as a tool to study the hydrodynamics of the concerned area. In order to set up an efficient model of the study area, a number of theoretical cases with different channel shapes will be analyzed at the beginning of the study. These theoretical cases will guide to understand the modelling steps and being familiar with the software itself. A tidal flat will be incorporated beside the channel in the theoretical model to check the flooding and drying event due to the tide.

A real model representing the study area will be developed after testing the proper functioning of theoretical model applications. The final case study will include the bathymetry of IJzer channel and DEM of neighbouring inter tidal zone with observed water level at Nieuwpoort. The model output will be compared with the campaign data of March 2003.

Flow velocity in the tidal flat is identified as the most important variable of this study. The spatial and temporal plots of velocity vectors in the tidal flat will indicate the present physical situation of the area. Velocities provide good indications of bottom shear stress and the process of sedimentation or erosion can be visualized from this study.

Other contributions of this research project are analysis of physical characteristics of IJzermonding which are obtained from ADCP and CTD measurements. GIS techniques will also be widely used in this thesis to interpolate and merge the bathymetry and DEM. GIS application will make the preparation of model data more convenient.

### **1.3 Scope of the study**

This study is the continuation of another thesis work at Civil Engineering Department in 2002-2003. The MATLAB script developed in that previous work to interpret the ADCP velocity measurement (*Caluwaerts, 2003*) has been updated. The physics behind the hydrodynamic processes in 'De IJzermonding' has been investigated in the present work. Further update of this thesis is also possible by adding the sediment transport module to this developed hydrodynamic model.

This thesis contains seven chapters, each with its own purpose:

- *Chapter 1* describes the objective and scope of this thesis.
- *Chapter 2* states the physical characteristics of the study area. The descriptions of the problems that need to be addressed in this thesis are also mentioned here.
- *Chapter 3* is designed for the data analysis that has been done during the pre-processing of model inputs and comparison of results.
- Description of TELEMAC software and the theoretical background of the model are described in *Chapter 4*.
- Set up of model with theoretical cases is mentioned in *Chapter 5*.
- The real case study and the results of the model outputs are shown in *Chapter 6*.
- The conclusions of this research and recommendations for further research are described in *Chapter 7*.

## Chapter 2: Characteristics of the Study Area

### 2.1 Study Area

The IJzer is the only river in Belgium which flows to the North Sea at Nieuwpoort. It is originated from Northern France and discharges in Western Flanders. This is a lowland slow moving river through agriculture field with a catchment area of 1101 km<sup>2</sup>. It has a total length of 76 km, of which 45 km lies in Flanders (Rycke *et al*, 2003). The left bank of IJzermondig is protected by dikes from the middle age and presently it is highly urbanized with holiday resorts. The right bank remains with natural character of sandy beach, mudflats, inter tidal zones and coastal dune until 20<sup>th</sup> century. The area of nature reserve of IJzermondig consists 103 ha of marsh land, the former naval base, the beach and the surrounding (Adam, 2004).

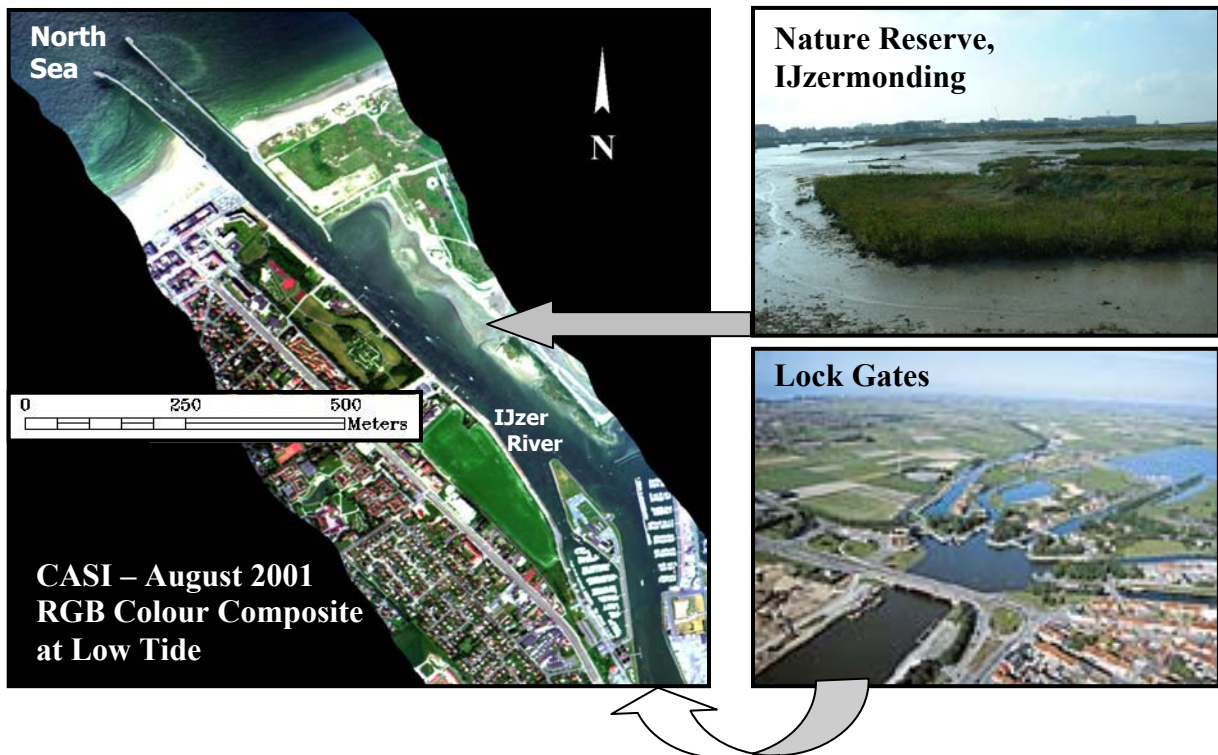


Figure 2-1: Study Area of 'De IJzermondig'

The study area in this thesis involves the estuary of the IJzer River. The lock gates are located 3.3 km from the North Sea. The main focus of the study involves in the nature reserve which is located up to the length of 1.7 km from the sea. The IJzer mouth is also considered up to this length in the model domain and the rest of the upstream part which consists the harbours and the lock gates are represented as rectangular reservoirs. The average width of the channel is 150m and with the tidal flat is 300m which varies according to the tide in the middle section of the model domain.

Near the mouth of the river the tidal influence of the sea is cut of by a large dam construction enabling an artificial water level management by sluices for shipping (AWZ, 1999). The study area is situated at the downstream of the sluices and subject to the periodic variation of the surface water levels of the North Sea. There are two high tides and two low tides each day. The two high and low tides each day are not of equal height due to the changing distance of the earth and the moon.

## **2.2 Flora and Fauna**

The mudflat is the bare muddy silt plate that floods twice a day at high-tide. The highly fertile clay particles that stay behind each time represent a banquet for millions of microscopic invertebrates and in their turn constitute the main source of food for numerous fish and birds. All year long one can find Oystercatchers and Shelducks here, looking for food at low-tide. The fish in turn attracts Cormorants, Red-breasted Mergansers and occasionally common seals. The tidal flat lies a bit more elevated, and are already covered with Sea-blite, Glasswort and Sea-Lavender. The inter tidal zone is criss-crossed with tideways, causing the sea to wash over it at spring tide. In the arid dune grassland plants as Large Thyme, Sticky Stork's-bill, Yellow Bedstraw, Squinancywort are growing. Among the birds, the Stonechat appears in the rougher parts, and the largest population of Wheatear can be seen in the entire coast (FRAME Project, 2003).

### **2.3 Brief History of 'De IJzermonding'**

A military harbour and a marina were established in the estuary of the IJzer River in 1950 and 1970. A huge amount of dredging sludge was produced during the construction phase of these harbours. This sludge (approximately 300,000 m<sup>3</sup>; detail of the map published by the National Geographical Institute, edition 1998) was dumped into the nearby tidal flat and dunes. It created a major environmental impact on estuarine ecosystem and natural habitat on the right bank of IJzer River.

In 1993 the Ministry of Defence announced that the Naval Base of Nieuwpoort would be alienated (*Deboeuf & Herrier, 2002*). In the framework of the Decree on the protection of the coastal dunes, the Flemish Government announced the former naval base as a 'protected dunesite' in November 1994. From 1995 the naval base area was referred as 'natural area with scientific value' in the town and country planning map. Severely degraded right bank of IJzermonding was designated as a part of a special protection zone in execution of the European "Bird-Directive" 79/409/EEC. In 1996, Flemish Government proposed the whole IJzer river mouth (including the naval base) as a candidate Special Area of Conservation in execution of the 'European Habitat Directive' 92/43/EEC (*Deboeuf & Herrier, 2002*). Since then the reserve is classified as 'landscape' and 'biologically very valuable' for the restoration of high natural values.

The Flemish government acquired the former naval base in 1998. The old naval base consists of heightened terrain, a slipway, docks and some infrastructure. The Universiteit of Gent developed a nature restoration project by the order of AMINAL. The restoration work was taken into action from 1999. The buildings, roads, docks and slipway were demolished (2000-2001) and the terrain was levelled to the original substrate (2001-2003). The aim of this project is to restore the natural gradients in the polder area. All these works resulted in the expansion of these biotopes to the dimensions of many times their former remnant and in the return of the jagged natural pattern of the transitions between each environment (*Adam, 2004*). In order to make it possible for people to enjoy all of this, the bicycle track and footpath has been rebuilt.

## 2.4 Problem Description

There are several physical conditions that will affect the feasibility of restoring inter tidal zones: presence of channels, availability of material for levees, pond subsidence, potential for flooding, and infrastructure impediments. In order to restore natural tidal flow to marshes, the proximity to tidal waters, the existence of channels and other factors must be considered. It will also be important to integrate the need for flood control levees with the levees required for wetland restoration.

Inter tidal zones are dynamic aquatic environment with specific flora and fauna. Their conservation is one of the major aims of the restoration project. Tidal flats responded more to the changes in driving forces such as sediment supply, wind or wave climate and tidal regime (Wal and Pye, 2004). These require extensive attention in the recent years due the sea level rise as a consequence of global warming. The estuarine wetlands may respond several ways subject to sea level rise. Sedimentation and erosion are the major factors to study for development of a tidal flat. Rapid erosion inter tidal zone is reported in some estuaries of Western Europe (Allen, 2000). Many biological and physical processes can disturb soft sediment habitat. This disturbance might occur in this study area at various intensities, frequency and spatial scales. In some cases marsh surface and vegetation are destructed and washed away with tidal current. In addition inter tidal zones are of high natural value providing a habitat for migrating birds and nursery for fishes. Erosion of mudflats is identified as one of the major problem in this study area.

The development of this nature reserve in IJzermonding is rather complex. The natural forcing factors and condition together with human activities have to be taken into account to understand and predict the development of this tidal flat. The spatial and temporal variation of flow velocity is required to investigate for adequate understanding of the underlying causes of the changes in the tidal flat. The issue of erosion of mudflat needs to be addressed with special attention in this dissertation thesis for the proper management strategy of restoration of the tidal wetland.

The laboratory for hydraulics of the Katholieke Universiteit Leuven is engaged for the monitoring of this nature reserve. A measurement campaign was performed in March 2003 to determine stream velocities in the IJzer channel. A similar study was done by *Caluwaerts* (2003) in the dissertation thesis of Civil Engineering in Katholieke Universiteit Leuven, in which a hydrodynamic model with hypothetical tides has been developed for the IJzermonding. This report is intended to provide hydrodynamic modelling of the area with real observed data. It can also assist for guiding further development of the sediment transport model of the study area.



## **Chapter 3: Data Analysis**

### **3.1 Reference System**

A reference datum is a known and constant surface which can be used to describe the location of unknown points. On Earth, the normal reference datum is sea level. As the sea level is not constant everywhere in the globe in particular due to the high or low tide, a reference datum is needed that represents the same surface or elevation of all points on the earth and that remains constant over time.

#### **3.1.1 WGS84 and ED50**

The datum used for GPS positioning is called WGS84 (World Geodetic System 1984). It consists of three-dimensional Cartesian coordinate system and an associated ellipsoid, so that WGS84 positions can be described as XYZ Cartesian coordinates or latitude, longitude and ellipsoid height coordinates. The origin of the datum is the Geo-centre (the centre of mass of the Earth) and it is designed for positioning anywhere on Earth.

Following the Second World War, survey data the central area of mainland Europe was used in a united adjustment to provide a common datum for military mapping in Europe. The completed work was known as the European Datum 1950 (ED50). The maps used in this study are referred to this system.

The surface elevation is expressed in TAW ('Tweede Algemene Waterpassing': The Belgian reference system for orthometric height constructed by water-levelling)

#### **3.1.2 UTM Projection**

As the earth is a sphere, any representation of its surface in a flat sheet of paper involves distortion. Over the centuries, various geometrical schemes have been worked out for

representing the curved surface of the Earth on map sheets; these schemes are known as map projections. All projections have certain advantages and disadvantages, and the selection of one or the other depends chiefly on the needs of the user. The size and shape of the country being mapped determines the most suitable projection for its system of topographic maps. The most convenient way is to divide into strips, usually called zones, which are projected onto a plane in orderly fashion. One such system of strip projection is the Transverse Mercator. It is called *transverse* because the strips run north-south rather than east-west along the equator, as in the standard Mercator projection. A special type of Transverse Mercator is the Universal Transverse Mercator (UTM) Projection.

In the case of this study, the bathymetry of the IJzermonding and DEM of surrounding area are also referred to UTM projection with ED50. The coordinate of the study area in the model is set up in the UTM system. The MATLAB programme developed which reads the measured velocity from ADCP gives the location in degree. For this reason the locations of the measured velocity obtained from the programme are converted into UTM projection of ED50 to incorporate it with the model output.

### 3.2 Bathymetry

Bathymetry data have been obtained from a field survey performed in July 2002 (Caluwaerts, 2003). This data cover the area from the IJzer mouth up to the lock gate. DEM of the right bank has been used concerning the topography of nature reserve.

**Table 3-1: Geographic Data Description**

Files	Description	Data Source	Reference Level	Data Density
DEM <sup>1</sup>	Elevation of the tidal flat area	Laser scanning by airplane	TAW <sup>2</sup>	1 point / 4m <sup>2</sup>
Bathymetry	Bathymetry of the navigation chanal	Ecosounder	MLLWS <sup>3</sup>	1 point / 25 m <sup>2</sup>

<sup>1</sup> DEM data's accuracy in height has a standard deviation of 5 cm

<sup>2</sup> Belgian Reference Level

<sup>3</sup> Mean Lowest Low Water Spring at Nieuwpoor

Both data have been collected from two different files that need to be merged in order to get the total information of the study area. This merged file has been used in the model to define the bathymetry of the domain. The properties of Bathymetry and DEM are described in Table 3.1

To merge the bathymetry and DEM point, one of the initial problems to solve is the difference in reference systems used in the two data sets. The bathymetry data is referred to MLLWS reference system while the DEM is in TAW. For the convenience of the data processing, the TAW reference system is chosen in the present study. Thus, the difference ( $\Delta Z$ ) between the two reference systems (MLLWS-TAW) at Nieuwpoort is added to the depth values of the bathymetry file to refer the whole domain in TAW. The relation between the two reference systems is explained in Figure 3-1.

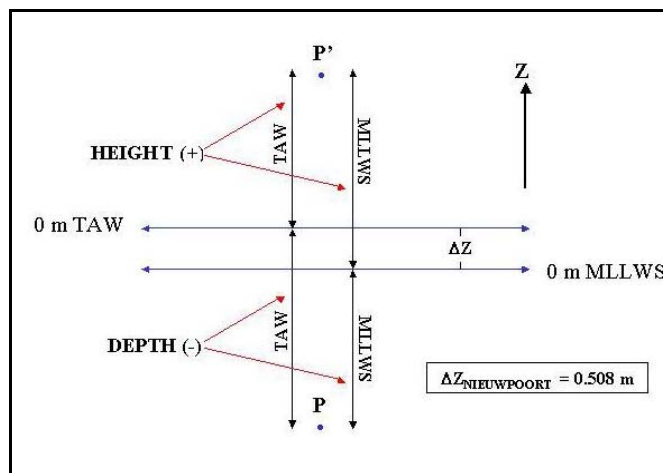


Figure 3-1: Relation between TAW and MLLWS Reference Systems at Nieuwpoort

### 3.2.1 Interpolation Method

The geographic data have some missing points in the mouth and an irregular and very dense distribution of points in the right bank of the domain. In order to get a more regular data point's distribution, the ArcView software has been used. The first step is to interpolate the missing points in the estuary. Three interpolators, IDW, Spline and TIN, available in the GIS environment have been applied in this study.

The Inverse Distance Weighted interpolator (IDW) assumes that each input point has a local influence that diminishes with distance. It weights the points closer to the processing cell greater than those farther away. A specified number of points, or optionally all points within a specified radius, can be used to determine the output value for each location.

Spline interpolator fits a minimum-curvature surface through the input points. It fits a mathematical function to a specified number of nearest input points, while passing through the sample points. This method is best for gently varying surfaces being not appropriate if there are large changes in the surface within a short horizontal distance, because it can overshoot estimated values.

The Triangulated Irregular Network (TIN) partitions a surface into a set of contiguous, non-overlapping, triangles. A height value is recorded for each triangle node. Heights between nodes can be interpolated thus allowing for the definition of a continuous surface. TINs can accommodate irregularly distributed as well as selective data sets.

### 3.2.2 Interpolation of Bathymetry

IDW and TIN interpolator's results show the best fit. Based on that, the TIN method has been chosen to interpolate the missing points in the domain. A new regular grid domain has been generated, with a grid size of 10 m.

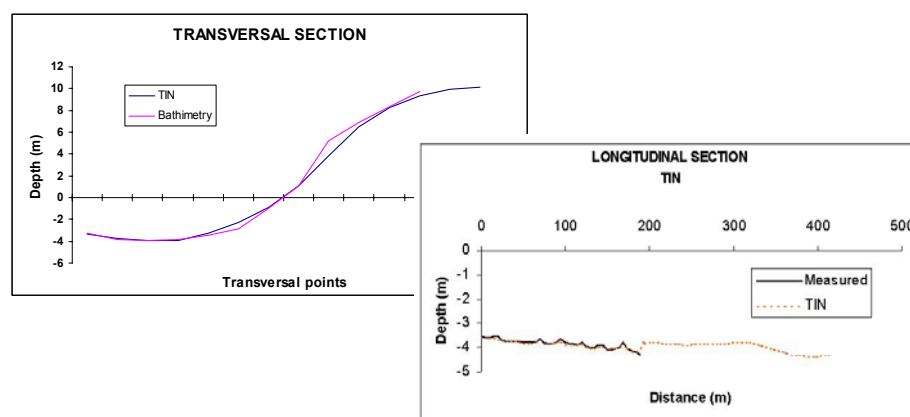


Figure 3-2: Interpolation Results

Topographic information about the area over the right bank of the estuary has been associated in the IJzer bathymetry. The final domain containing the channel bathymetry and neighbouring topography is shown in Figure 3.3. The upstream ends of the canal, harbour and lock gates have been replaced by a big reservoir to balance the volume of the domain. The same principle is applied to replace a small harbour present in the area by another reservoir.

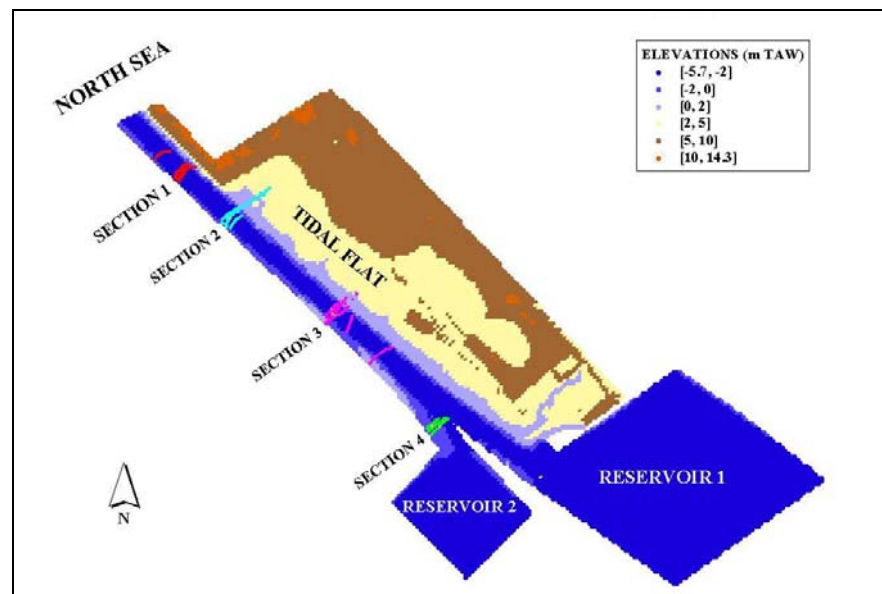


Figure 3-3: Model Domain

### 3.3 Tides

A M2 tide, the main semidiurnal lunar tide due to the mean motion of the moon, is used for a first theoretical approach. The semidiurnal is the dominant tidal component in most of the world's oceans, being also characteristic of the North Sea coast in Belgium, where each tidal cycle has a period of approximately 12 hours and 25 minutes with mean amplitude of 2.25m. The theoretical tide is generated in the form of wave equation,  $A \sin \omega t$ . The amplitude ( $A$ ) of the wave is taken as 2.0, 2.25 and 2.5 for the neap, mean and spring tide respectively. The angular velocity is calculated according to the relation,  $\omega = 2\pi / T$ , where  $T = 12.42$  h. These theoretical tides are used as the liquid boundary file in the application of theoretical case studies. Water level measurements are also available at the mouth of the IJzer River at an interval of 5 minutes, while time registered in GMT. The data of March 2003 is taken from

the set to simulate the real case model. The general pattern of the tide shows that the rising event during the spring tide of 19<sup>th</sup> March, takes 5 hours to reach the peak and 7 hours for the ebbing event.

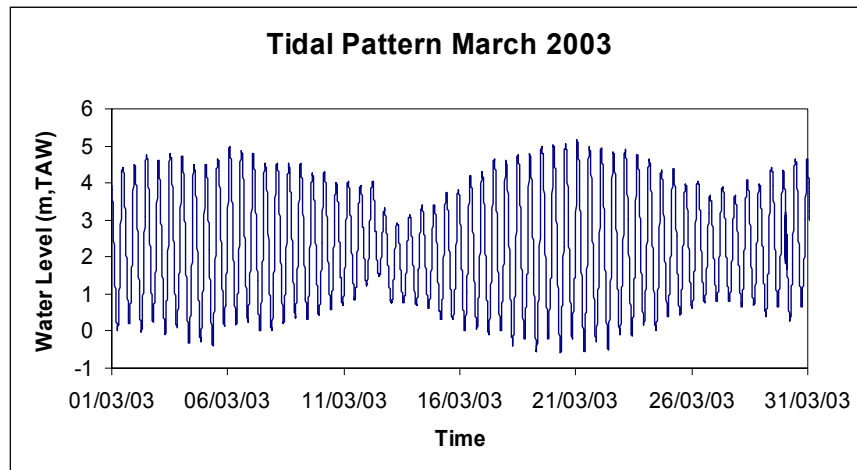


Figure 3-4: Time Series of Tidal Cycle

### 3.4 ADCP & CTD Measurement

To understand the sedimentation process in 'De IJzermonding', ADCP and CTD measurements have been collected during the field campaign of March 19, 2003. Flow velocity measured by ADCP has been collected from four cross-sections shown in Figure 3-3 as well as longitudinally at the Ijzer Estuary. It covers one tidal cycle of flood current and ebb current which is shown in the Figure 3-5. ADCP data have been analysed in this study mainly to compare the model output of flow velocity.

The hydrographic data for the study are derived from Conductivity, Temperature, Depth (CTD) sensors. CTD generates continuous profiles of four different variables: pressure (db), temperature (deg C), salinity (PSU), density ( $\text{kg/m}^3$ ). Each profile, consisting of the depth and associated measured variables, is stored with depth increasing monotonically downwards. The measured data are analysed by SEASAVE software shown in the Figure 3-6. The physical characteristics of water in this location are obtained from this analysis. The water temperature has been recorded as 7<sup>0</sup>C during the campaign. The salinity and density ranges vary along the vertical profile during the changing period of flooding and ebbing, but remains constant along

the depth during the slack period. Water is well mixed in the slack period and the density of water is homogeneous in the vertical profile for the slack period.

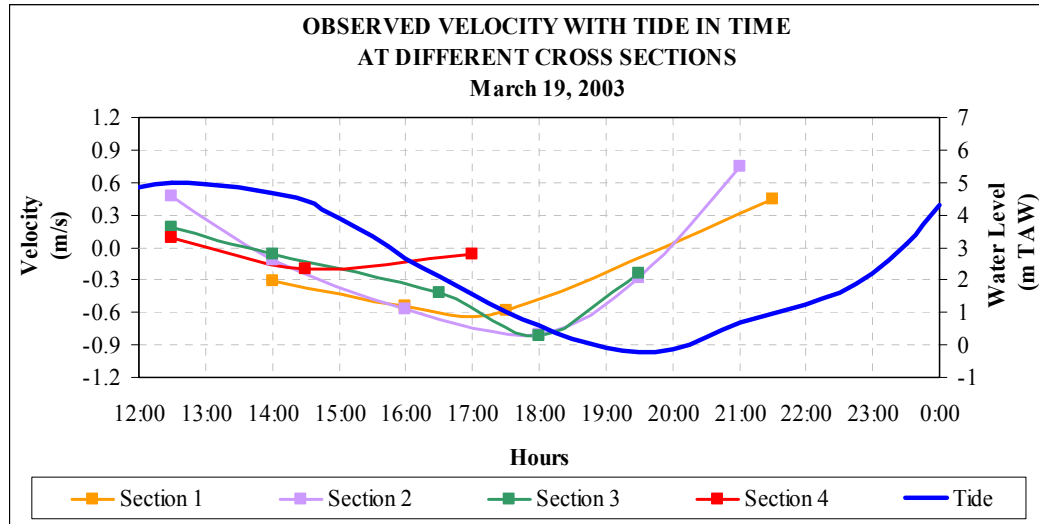


Figure 3-5: Comparison of Flow Velocity at Different Sections of the IJzer Mouth Measured by ADCP

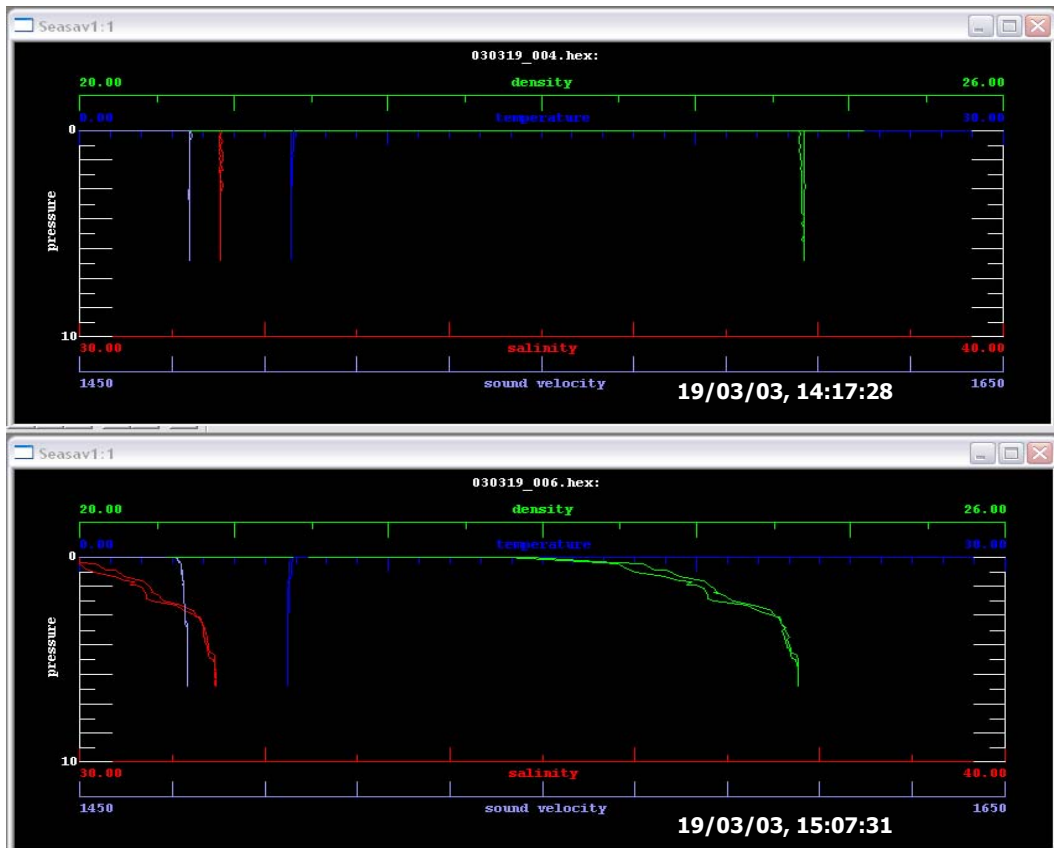


Figure 3-6: Processing of CTD Measurements with SEASAVE Software

## Chapter 4: TELEMAC-2D Software

### 4.1 TELEMAC-2D System

TELEMAC-2D is developed by the National Hydraulics and Environment Laboratory (Laboratoire National d'Hydraulique et Environnement – LNHE) of the Research and Development Directorate of the French Electricity Board (EDF-DRD). It has been developed as part of complete computational software called the TELEMAC system. This offers all the modules required for 2D numerical simulations in hydrodynamic, sediment transport and water quality modelling.

The modelling system for a 2D-hydrodynamic simulation is shown in Figure 4-1. MATISSE, STBTTEL, TELEMAC2D and RUBENS constitute the four modules used by TELEMAC-2D during the modelling process.

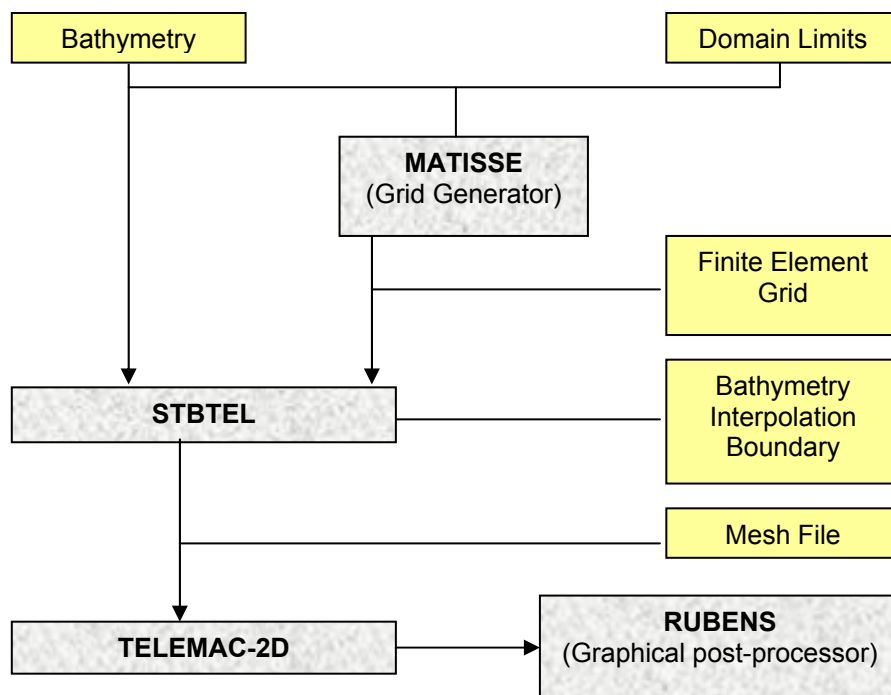


Figure 4-1: 2D-Hydrodynamic Modelling in TELEMAC System



## 4.2 2D Hydrodynamic Simulation in TELEMAC

TELEMAC-2D uses The Finite Element (FE) technique to solve the shallow water equations, continuity and momentum, for every node within the domain. Substitution of the continuity equation in the two momentum equations (two horizontal components of the depth-average velocity) leads to the non-divergent form of the momentum equation. The main results at each node of the computational domain are the water depth (H) and the horizontal components of the depth-average velocity (U, V) per time step.

A linear interpolation between the surrounding nodes is performed in order to compute solutions for no-node points where variables are defined as the sum of the nodal values multiplied by the interpolation functions. If the solution or the physical data is varying rapidly compared with the distance between nodes, accuracy can be improved by grid refinement.

The domain characteristics are defined in MATISSE, through the grid generation. STBTTEL converts the geometry and the boundary information into the TELEMAC format in order to solve the hydrodynamic equations, through the use of the finite element method. The numerical computation results can be visualized in RUBENS, the graphical post-processor of the system.

### 4.2.1 Model Assumptions

In order to build the two-dimensional model, TELEMAC-2D simplifies the *Navier-Stokes* equations to *Depth Averaged Shallow Water Equations (SWE)*. The fluid is assumed to be Newtonian, incompressible and vertically homogeneous. Horizontal density variations are considered through the *hypothesis of Boussinesq*, which ignores the density variations except insofar as they give rise to a gravitational force (*Boussinesq*, 1903). Therefore, the density profile  $\rho_0(z)$  is replaced by its vertically averaged value  $\rho_0$ . For the long wave approximation adopted, the pressure distribution is assumed to be hydrostatic (the vertical pressure gradient is balanced by the gravity acceleration).

## 4.2.2 Hydrodynamic Equations

The TELEMAC-2D code solves the second-order partial differential equations for depth-averaged fluid flow derived from the full three-dimensional Navier–Stokes equations. They are also called the Barre de Saint-Venant Equations. This gives a system consisting of an equation for mass continuity and two force-momentum equations. The equations at constant density are averaged over the vertical by integrating from the bottom to the surface. The averaged form of the continuity equation is:

$$\frac{\partial h}{\partial t} + \frac{\partial(hu)}{\partial x} + \frac{\partial(hv)}{\partial y} = 0 \quad (4.1)$$

The average form of the momentum equations are:

$$\frac{\partial(hu)}{\partial t} + \frac{\partial(hUU)}{\partial x} + \frac{\partial(hUV)}{\partial y} = -gh \frac{\partial Z}{\partial x} + \frac{\partial}{\partial x} \left( hv_e \frac{\partial U}{\partial x} \right) + \frac{\partial}{\partial y} \left( hv_e \frac{\partial U}{\partial y} \right) + hF_x \quad (4.2)$$

$$\frac{\partial(hv)}{\partial t} + \frac{\partial(hVV)}{\partial y} + \frac{\partial(hUV)}{\partial x} = -gh \frac{\partial Z}{\partial y} + \frac{\partial}{\partial x} \left( hv_e \frac{\partial V}{\partial x} \right) + \frac{\partial}{\partial y} \left( hv_e \frac{\partial V}{\partial y} \right) + hF_y \quad (4.3)$$

where  $U$  and  $V$  are depth average velocity components in  $x$  and  $y$  Cartesian directions,  $h$  is the depth,  $v_e$  is the coefficient of momentum diffusion ( $\text{m}^2\text{s}^{-1}$ ),  $g$  is the gravitational acceleration,  $t$  is the time,  $Z$  is the elevation of free surface (m),  $F_x$  and  $F_y$  are some source term of the momentum equation in  $U$  and  $V$ , respectively, which include friction, coriolis, and wind force.

The bed friction is represented as quadratic function of velocity,  $\vec{\tau} = \rho C_f |U| \vec{U}$ ; where  $\vec{U} = (U, V)$ . The friction coefficient ( $C_f$ ) can be parameterised either in terms of Chezy ( $C$  in  $\text{m}^{1/2}\text{s}^{-1}$ ), Manning ( $m$  in  $\text{m}^{1/3}\text{s}^{-1}$ ), or Nikuradse ( $k_s$  in mm) friction coefficients applying the respective equations.

$$C_f = g / C^2 \quad (4.4)$$

$$C_f = \frac{gm^2}{h^{1/3}} \quad (4.5)$$

$$C_f = 1/32 \left\{ \log \left( \frac{14.8h}{k_s} \right) \right\}^2 \quad (4.6)$$

Simulation involving the calibration of model prescribes a range of values for  $C$ ,  $m$  and  $K_s$ . TELEMAC-2D considers solid boundaries in order to solve the basic equations. These solid boundaries illustrate that: (1) no mass flux of water occurs through the bottom and closed lateral faces ( $\vec{U} \cdot \vec{n} = 0$ ), where  $\vec{n}$  is the unit normal vector of the boundary, (2) there is a free slip condition at the wall of all vectors tangent ( $\vec{t}$ ) to the wall ( $\partial(\vec{u} \cdot \vec{t}) / \partial n = 0$ ), (3) the friction condition at the bed written as ( $\partial(\vec{u} \cdot \vec{t}) / \partial n = \alpha(\vec{u} \cdot \vec{t})$ ), where  $\alpha$  is the friction coefficient provided by the user.

TELEMAC-2D solves the equations on non-structured grids, with triangular finite elements. The nature of the finite element mesh allows the fitting of various sized elements within a specified boundary, which allows high resolution in areas of increased bed slope or narrow channels and low resolution in areas where detail is not required (*Fernandes, 2002*).

The Navier–Stokes equations are solved based on the operator-splitting method (*Marchuk, 1975*), whose main principle is that the hyperbolic and parabolic parts of the Navier–Stokes equations should be treated separately, in order to use well adapted numerical methods for each part. The solution involves two steps: (1) solution of advection terms, (2) solution of the propagation, diffusion and source terms. The method of characteristics has been applied to solve the advection of  $U$  and  $V$  (*Galland et al., 1991; Bates et al., 1997; Bates et al., 1998*). The streamline upwind Petrov–Galerkin method (SUPG) has been applied to solve the advection of  $h$  (*Brookes and Hughes, 1982*). The propagation, diffusion and source terms are solved by the finite element method, where an implicit time discretisation allows the elimination of the non-linearity in the equations. Variation in the formulations and space discretisation transform the continuous equations into a linear discrete system where the

values of  $h$ ;  $U$  and  $V$  at the nodes are the unknown variables. This system is solved by an iterative conjugate gradient method (Hervouet and Van Haren, 1994).

### 4.3 Model Inputs

TELEMAC-2D reads physical and numerical inputs given by the user in the *Steering file*, known as the control panel of the system. The steering file comprises a number of keywords, which values are assigned according to the physical condition of the area. It has the links to external files, which contains information about the grid definition of the domain and imposed boundary conditions created in MATISSE as geometry and boundary files respectively.

#### 4.3.1 The Mesh Generation

The creation of the mesh is the first step to be taken during the modelling process in order to define the nodes where the computation of the model variables takes place. MATISSE allows the generation of triangulated irregular mesh which dimensions are defined by the user in TELEMAC system. This is a great advantage of the system since a more realistic representation of the domain can be done, allowing more detail in areas where it is needed.

Five different modes are available in MATISSE for the mesh generation. The *Bathymetry*, *Geometric Lines*, *D.E.M.*, *Mesh* and *Boundary Conditions* modes are chosen accordingly in order to build successfully the grid domain.

Once a new project is created, the *Bathymetry* mode allows the user to create or import the bathymetry in the project area and to define the limits of the domain and the coordinate system.

The computational domain must be defined by identification or creation of contour lines in the *Geometric Lines mode*. These lines, natural or arbitrary, will work as a support for the distribution of the nodes in the grid.

The *D.E.M.* mode, the environment in which the user defines the inter-node distance criteria, allows for different grid size definition in the domain to give more detail in more needed areas.

The mesh generation is performed in the *Mesh* mode. The defined characteristics of the domain can be imported into the TELEMAC-2D simulation through the generation of a

geometry file in Serafin format at the end of the process. Moreover, new constraints can be taken into account or manually modifications in the mesh can be made afterwards.

After the complete definition of the mesh, a definition of the boundary conditions for each homogeneous segment of the border will be performed inside the *Boundary Conditions* mode. The points sharing the same boundary definition are associated and defined as groups.

The parameters' characteristics along the different boundary sites are defined using entities to be linked afterwards with the corresponding boundary group. A boundary file to be imported during the simulation will be generated as the last step.

### 4.3.2 Boundary Conditions

Physically, the boundary conditions of the domain of calculations can be liquid or solid. An impermeable condition exists for the solid boundaries, which does not allow discharge across the boundary. The liquid boundary is a difficult case to deal with because it supposes the existence of fluid domain that does not form part of the calculation domain but one that can nevertheless influence it. This influence has to be translated into boundary conditions. In order to deal with this, the system asks the user to indicate for each of the principal variables of the code (variables H, U and V) if it is prescribed or free. This has to be indicated for each point of a liquid boundary.

Therefore, boundary conditions are prescribed essentially in two steps in TELEMAC. At first the definition of entities at the boundaries in MATISSE; these information is stored in the *Conlim File* and is read at the beginning of the computation. Each line of this file is dedicated to one point of the mesh boundary and codes are used to identify the conditions set for every printout variable. In a second step, the prescriptions of the values for water surface elevation in the domain are generated based on the amplitude and tidal phase reads in the liquid boundary file.

## 4.4 The Numerical Schemes

TELEMAC-2D allows various numerical schemes for the advection of the velocity (U, V), depth (H), tracer (T) and k-epsilon variables (k-Epsilon turbulence model) which is free choose according to the use of model. There are five advection schemes, each of which applies to a variable that is advected (in the order: velocity, depth, tracer, k-epsilon).

1. Method of characteristics
2. "Streamline Upwind Petrov-Galerkin" (S.U.P.G.) scheme with several variants
3. "Hybrid" scheme with several variants
4. FCT (flux-corrected transport)
5. Variants of S.U.P.G. applied to the continuity equation

The TELEMAC-2D time discretisation is semi-implicit. Selecting the type of advection gives access to schemes with widely varying properties for mass-conservation and numerical stability. The theory behind every scheme mentioned is well explained in the TELEMAC-2D Formulation Document. The advection scheme is defined in the Steering file using the keyword: "TYPE OF ADVECTION".

TELEMAC-2D offers the possibility of mass lumping on the mass matrices involved in computing the matrices for depth and for velocity. This technique means bringing some or the entire matrix on to the diagonal, and enables computation times to be shortened considerably. However, the solution obtained is very much smoothed.

The rate of mass lumping is fixed with the keywords "MASS-LUMPING ON H", "MASS-LUMPING ON VELOCITY". The value 1 indicates maximum mass lumping (the mass matrices are diagonal) and the value 0 (default value) corresponds to normal processing without mass lumping. More details are given in the TELEMAC-2D Formulation Document.

#### 4.4.1 The Courant Number Management

The Courant number is defined as the number of grid cells crossed by a water particle during a time step,  $\sigma = C\Delta t / \Delta x$ , where  $C$  is the propagation velocity. For long waves the celerity is defined by,  $\sqrt{gh}$ ; where  $g$  and  $h$  are the gravity coefficient and the water depth respectively.

During a model simulation, the Courant number value considerably influences the quality of the results. The numbers above 7 or 8 produce poor quality results, for numerical schemes without a stability condition on the Courant number (Telemac User's Manual).

#### 4.4.2 The Turbulence Model

TELEMAC-2D offers four options of different complexity for the modelling of turbulence. The key word related with this feature is "TURBULENCE MODEL". A Reynolds decomposition and stochastic averaging is applied. Reynolds shear stresses resulting from this process are modelled as proposed by Boussinesq by using a turbulent viscosity.

There are different assumptions that can be made to estimate the viscosity value (molecular and turbulent effects). An isotropic depth mean value is taken if a *constant viscosity coefficient* is assumed. In other hand, the *Elder model* assumes a non-isotropic velocity dependent depth mean viscosity value (variation along and across the velocity direction).

For the *Smagorinski model*, the eddy viscosity is proportional to the square of the characteristics filter length introduced by the grid discretisation and the modulus of the large eddy strain rate; while for the *k-Epsilon model* it is a value computed thanks to the transport model of a turbulent quantity  $k$  (turbulent kinetic energy) and Epsilon (turbulent dissipation).

#### 4.4.3 The Friction Law

The Bottom friction in TELEMAC-2D can be modelled using a linear or a non-linear law. The first option is rarely applied because does not represent the reality. The friction is a quadratic function of the velocity and is well represented by the *Chezy*, *Strickler* and *Nikuradse* friction laws.

The friction law have to be defined by the user in the Steering file. The friction coefficient can either be provided by the user or determined by the turbulence model. If the first option is taken, the coefficient entered will depend on the law selected, being its value a function of the physical characteristics of the channel.

The key words concerning friction at the bottom are “LAW OF BOTTOM FRICTION” and “FRICTION COEFFICIENT”. A more detailed description of the equations and the assumptions taken for every law is given in the TELEMAC-2D Formulation Document.

#### **4.5 Treatment of the Tidal Flats**

The tidal flats are the areas besides the estuary that are periodically wet by the rising in water level during rising tide, becoming dry at low tide. TELEMAC-2D offers three different ways to process tidal flats to avoid parasitic driving terms generated in the exposed areas that otherwise would be taken into account by the program during the calculations.

In the first case, the tidal flats are detected and the free surface gradient is corrected. Areas of negative water depth are smoothed in order to prevent appearance of spurious solutions (Figure 4-2).

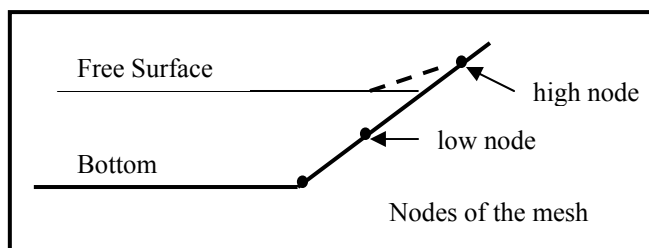


**Figure 4-2: Free Surface Gradient Correction Method**

The second treatment consists of removing from the calculations all the elements, which are not entirely wet. Masking of exposed elements option will assign a value of 1 to the wet elements and 0 to the dry ones (even partially dry). The contributions of the elements are multiplied by the mask, which in effect amounts to removing certain elements. This option has the advantage of saving computation time.



In the third case, processing is done in the same way as in the first case, but a porosity term is added to half-dry elements. Consequently, the quantity of water is changed and is no longer equal to the depth integral over the entire domain but to the depth integral multiplied by the porosity.

## **4.6 Model Output**

Three types of output files may be generated by TELEMAC at the end of a successful simulation: the result file, the listing printout and the formatted boundary and binary data file.

The result file contains all the information about the mesh geometry and the calculated values for all the printout variables and all the mesh points at each printout time step in a serafin format. The first graphic printout time step can be defined in the Steering file. The result file can be converted into an ASCII format by using a FORTRAN script.

During the model computation, TELEMAC-2D displays the listing printout of the current time step, the mass balance in the domain and the error involved in its calculation. The starting time for listing printouts is defined by the user in the Steering file. The formatted boundary and binary data files can be used to provide data to the programme as well.

### **4.6.1 Rubens: the Graphical Postprocessor**

RUBENS is a graphic visualization software package that allows the graphical post processing of the simulation results. Results of experimental measurements made at several single points of a one-dimensional space or on a two-dimensional space can be visualized in a structured or unstructured meshes made up of triangular or quadrilateral elements.

It includes a comprehensive range of functions. The user can define accurately the features and the aspect of the graphs. Moreover, new variables based on the defined printout variables could be defined easily in the software (i.e. the velocity vector).

## **Chapter 5: Methodology of Hydrodynamic Modelling**

### **5.1 Introduction**

In order to build the 2D-Hydrodynamic model of the IJzer estuary, four theoretical characterizations of the domain have been tested at the beginning of the study. The purpose of the theoretical cases developed by ideal tide and geometry are to be familiar with the TELEMAC-2D modelling system and establish feasible parameters of the model. The experience from these ideal cases, will guide the set up of the real case with real digital elevation model and liquid boundary condition at the mouth of the IJzer River.

### **5.2 General Model Settings**

#### **5.2.1 Geometry Definition**

The definition of the geometry of the domain is based on the elevation data imported at the beginning of the mesh generation process in MATISSE. The elevation data files used for the ideal channel modelling has been taken from a previous thesis work developed by *Caluwaerts* (2003), in which TELEMAC-2D was also applied.

For all the cases, a minimum inter-node distance of 10m has been defined in the mouth of IJzer to have a higher resolution for more accuracy and computation nodes near the open boundary. In the reservoir area the grid size has been set up to 50m to reduce the computation time, while a 20m node distance criterion has been established in the rest of the modelling domain.

### 5.2.2 Initial Conditions

The free surface elevation in the domain is considered at constant elevation; therefore the water depth at each point is calculated as the difference between the bottom elevation and the free surface elevation in the domain (User manual); both of them are referred to TAW.

The liquid boundary file that prescribes the water level at the liquid boundary along the simulation has been defined and read by TELEMAC-2D in the Steering file. The initial free surface elevation in the domain is assumed at the same level as in the open boundary side.

### 5.2.3 Boundary Conditions

The definition of the boundary sides and their physical characteristics has been established during mesh generation. A physical open boundary side has been considered at the mouth. An imposed water level (H) is defined at the open boundary side for all cases (Figure 5-1). A liquid boundary file with imposed water level values for a period of three days (ideal and real time series) has been prescribed to simulate the tidal dynamics in the estuary. A free liquid boundary condition is set for the horizontal velocity components (U, V).

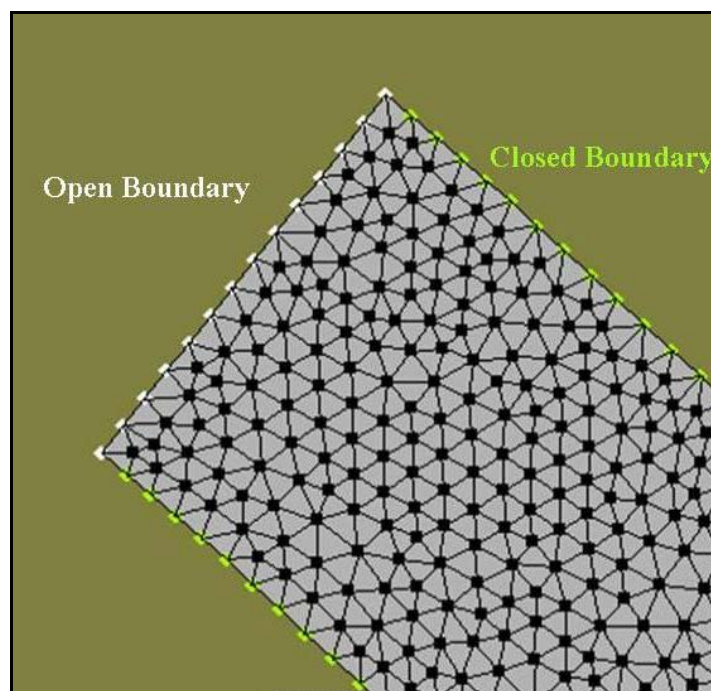


Figure 5-1: Boundary Definition

The rest of the points in the contour of the domain are considered as part of the close boundary, with a sliding condition set up for all the parameters (H, U, V, and t). A reservoir has been set at the upstream part of the estuary (close boundary) to balance the water volume in the domain for all the cases using an ideal geometry.

#### 5.2.4 The Friction Law

In narrow estuaries, where the flow is influenced everywhere by the banks or sidewalls, turbulent dispersion can play the dominant role as the energy dissipation mechanism. This is not the case when the transversal extension of the flow domain is large and the energy dissipation is controlled by the bottom friction (*Malcherek, 1999*). Due to the presence of inter tidal zones in the model domain, the estuary could be considered as a wide one where the energy dissipation is basically controlled by the bottom friction. Therefore, a good estimation of the friction coefficient value will have a determinant effect on the performance of the velocity modelling.

In the present study, the Chezy's coefficient is chosen as law of bottom friction. This coefficient depends basically on the hydraulic radius of the estuary. Based on the channel geometry and the water depth, a friction coefficient of  $65 \text{ m}^{1/2} \text{ s}^{-1}$  has been estimated for the real bathymetry. Due to the similarities in size between the real and the ideal geometries, this value has been assumed for the ideal cases as well. The model trials with different Chezy's coefficient have negligible impact on the flow velocity outputs in this relatively small domain.

#### 5.2.5 Numerical Options

The variables defined for graphic print outs in all the cases are the east (U) and north (V) velocity components, the free surface elevation (S), the water depth (H), the flow rate (Q), the bottom elevation (B) and the scalar velocity (M). The printout of the results for all the variables has been set for every thirty minutes to demonstrate the response of the system to the tide influence.

A simulation of three days has been carried out which is the same period for the water level time series imposed at the open boundary side. The time step has been chosen considering the

optimum computation time and the Courant condition to avoid instabilities and poor quality of results due to high values. A velocity of 10 m/s has been estimated for the tide celerity inside the channel for a water depth of 10 m (expected at high tide). This assumption was taken in order to reduce the risk to exceed a courant number of 7 (see chapter 4).

The constant viscosity option, which assumes the turbulent viscosity is constant through out the domain, has been chosen for the modelling of the turbulence in the estuary. The keyword "VELOCITY DIFFUSIVITY" that represents the overall viscosity coefficient for this option (molecular & turbulent viscosity) has a definite effect on the extent and shape of recirculation. Small viscosity values tend to dissipate only small eddies, whereas higher ones will tend to dissipate large recirculation. In the present study, its value has been defined to consider the expected recirculation processes in all models. The minimum value for this feature is  $1.10^{-6}$  m<sup>2</sup>/s corresponding to the molecular viscosity of water, being the default value of  $1.10^{-4}$  m<sup>2</sup>/s.

The mass balance is checked over the entire domain every simulation. This option allows computing the flows through the boundaries of the domain (liquid or solid) and the relative error on mass-conservation for each time step. The methods of characteristics (1) and conservative scheme & SUPG (5) have been chosen to solve the advection step for the velocity components and the water depth respectively. The accuracy for the resolution of the propagation step has a default value of  $1.10^{-4}$ . A higher accuracy would increase the computation time (reference manual).

### **5.3 2D-Hydrodynamic Model for Ideal Channels with an Ideal Tide Influence**

#### **5.3.1 Model 1: Rectangular Canal with a Reservoir**

The first domain implemented for a hydrodynamic simulation is a rectangular channel, with a single reservoir upstream and a liquid boundary at the mouth (*Caluwaerts, 2003*). The simplicity and symmetry of the area allows evaluating the performance of the model to show the hydrodynamic response of the system to validate initial assumptions for more complex cases.

The bottom surface elevation has been assumed at 0 m TAW everywhere (see Figure 5-2). A mesh of 2698 nodes has been generated in MATISSE covering a domain of 932,000 m<sup>2</sup> (633,000 m<sup>2</sup> for the reservoir area). A length of the IJzer mouth is considered as 2.3 km in the model.

An initial water elevation of 3.5 m TAW has been set for the whole domain. This value corresponds to the first water level read at the tide data file and will be used for all the models using an ideal tidal sign. The time step has been set every 5 seconds for all the models based on an ideal geometry. The default value of the velocity diffusivity has been kept for the present model (1.10<sup>-4</sup> m<sup>2</sup>/s). The accuracy for the resolution of the propagation step is fixed at 1.10<sup>-4</sup>, which is also the default value in the model. The results have been plotted in Rubens after the simulation.

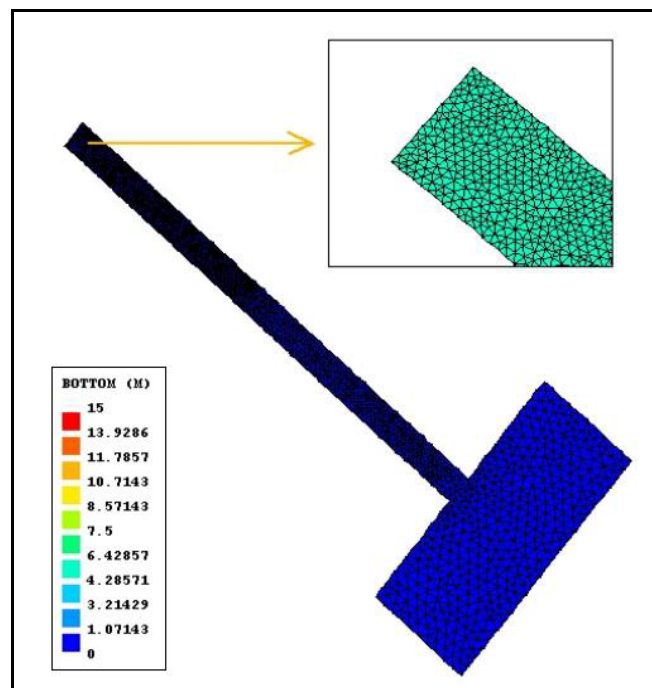


Figure 5-2: Domain of Model 1

Figure 5-3 and Figure 5-4 (result plots) show the spatial distribution of the free surface elevation and the velocity vector distribution in the estuary as well as the velocity components variation along the time for a point in the middle of the channel. From these plots, a six hours transition period is identified (half of the tidal period range imposed). It can be noticed as well that the velocity magnitude during ebb and rising tide is not the same in spite of the

symmetry precondition imposed for tide. The spatial pattern of velocity is not symmetric near the open boundary, although the domain geometry is rectangular. The phenomenon has been pronounced by the tidal effect, especially when the tide is rising. Higher velocity magnitudes are obtained during rising tide, being the highest on the left boundary side of the mouth.

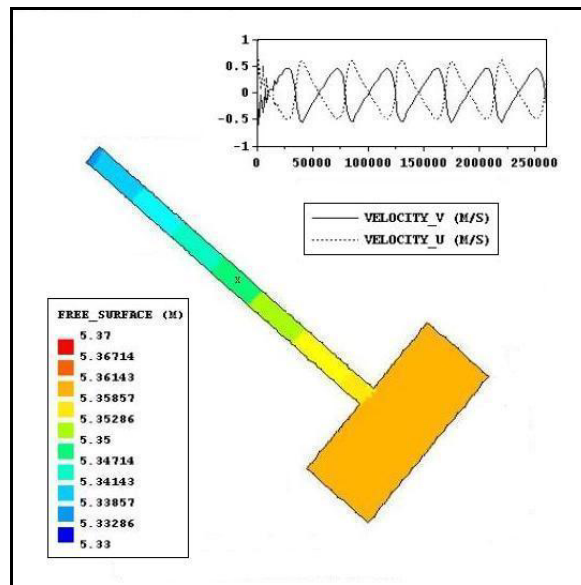


Figure 5-3: Model Results - Velocity Components and Free Surface Elevation

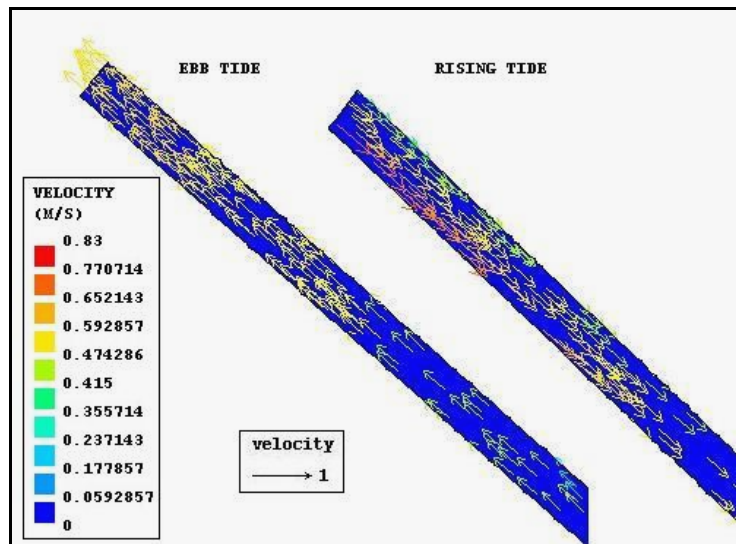
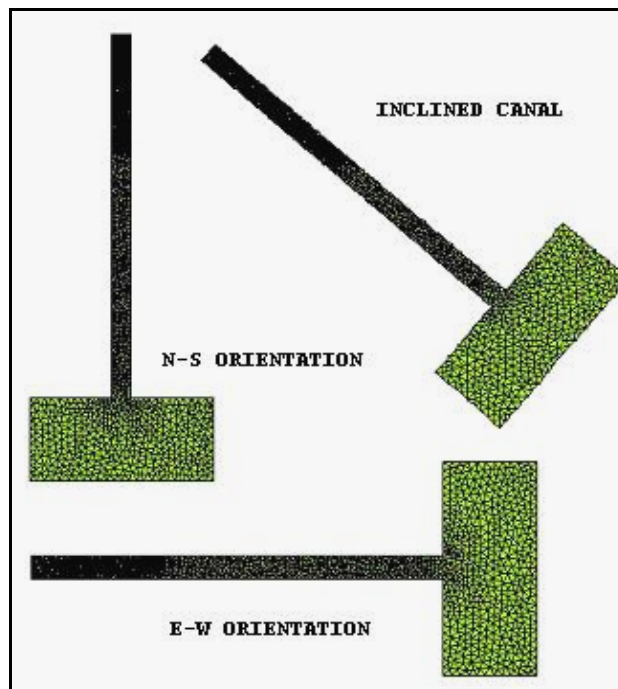


Figure 5-4: Model Results - Velocity Distribution in the Channel

The present situation has also been documented by *Caluwaerts* (2003) in his thesis document where a possible explanation for this unexpected behaviour is attributed to the fact that the

open edge is not directed parallel and perpendicular to the east and north axis of TELEMAC-2D. The effect on the velocity component could be due to the diffraction process of the water which is coming inside the river at the side of the wall near the open edge.

In order to search for some software limitations for the orientation of the domain, two new rectangular domains are analysed keeping the same size and shape, but changing its orientation to E-W and N-S (Figure 5-5).



**Figure 5-5: Model Results - Variations in the Orientation of the Model 1**

It can be noticed from the results of the new canal orientations shown in Figure 5-6, that the asymmetry problem of the velocity at the mouth has almost disappeared at the rising tide. However, high velocities are obtained at the mouth of the N-S orientation, which are not noticed in the E-W orientated model domain.

The results obtained using N-S and E-W oriented canals for the simplest model domain partially solves the asymmetry distribution of the velocity in the cross section. Nevertheless, the hypothesis about software limitations related to the orientation of the domain still remains uncertain and a more detailed research is advised.



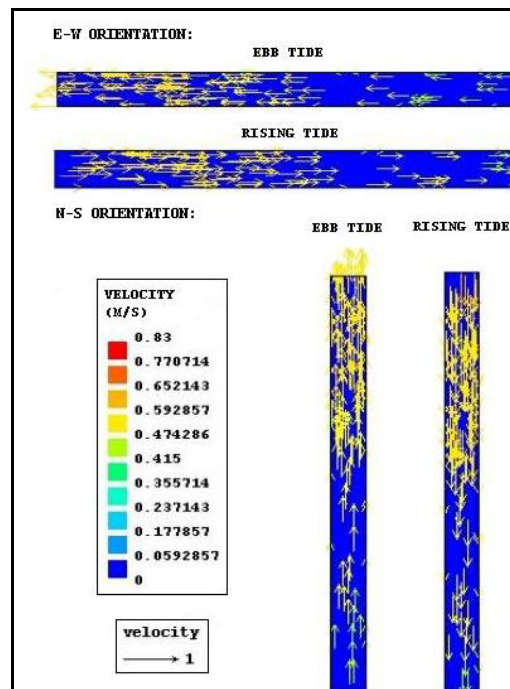


Figure 5-6: Model Results - Velocity Distribution of the North and the East Oriented Canals

### 5.3.2 Model 2: Rectangular Channel with a Side Basin and a Reservoir

A side basin has been added to the main canal to model the recirculation processes in the domain (Figure 5-7). A bottom elevation of 0 m TAW has been assumed for the whole domain (Caluwaerts, 2003). The initial water elevation of 3.5 m TAW has been kept in the domain and at the open boundary side. The depth in the model domain varies between 1.25 to 5.75 m according to tides.

The number of nodes in the domain defined in MATISSE during the mesh generation is 2,977. They are representing an area of 1,141,145 m<sup>2</sup> (460,310 m<sup>2</sup> for the reservoir area), which is a little bigger than the first model domain. The velocity diffusivity value has increased to 1.10<sup>-3</sup> (m<sup>2</sup>/s) to account for recirculation in the side basin, and the solver accuracy has been reduced to 1.10<sup>-3</sup> in order to keep suitable computation time.

The recirculation pattern in the side basin of the domain is well represented by the model (Figure 5-8). It is mainly present during rising tide as it is expected naturally. Moreover, lower velocities are obtained in the wider part of the mouth while the highest are present at

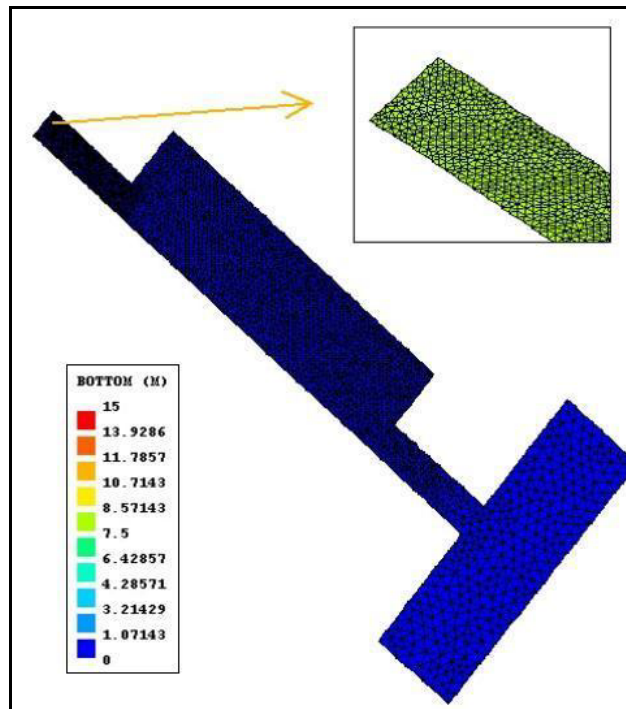


Figure 5-7: Domain of Model 2

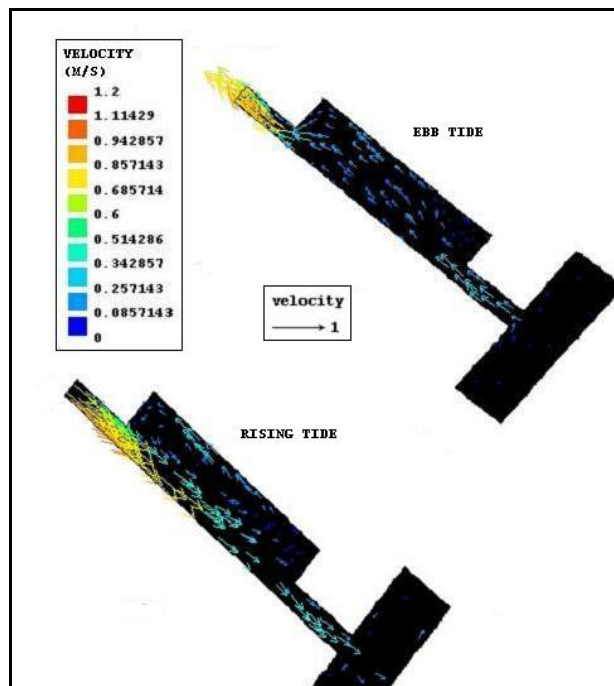


Figure 5-8: Model Results - Velocity Distribution at the Domain

the narrow mouth. These satisfactory results allow further implementation of a varying bottom elevation in the side basin area to account for the presence of inter tidal zones.

### 5.3.3 Model 3: Rectangular Canal Considering Tidal Flats and a Single Reservoir

A side basin with bottom slope of 0.031 m/m has been implemented (Figure 5-9). This new characteristic of the domain has been considered not only for natural recirculation processes but also the exposed elements of the grid (natural tidal flats), which will be wet during rising tide.

The grid domain accounts for a total of 3081 nodes. The model area covered by Model 2 has been applied as well to the present model application. The bottom elevation in the domain is 0 m TAW everywhere, except for the tidal flat side (*Caluwaerts, 2003*). The depth of the side basin varies spatially between 0 to 5.75 m depending on the position in a cross section and the time.

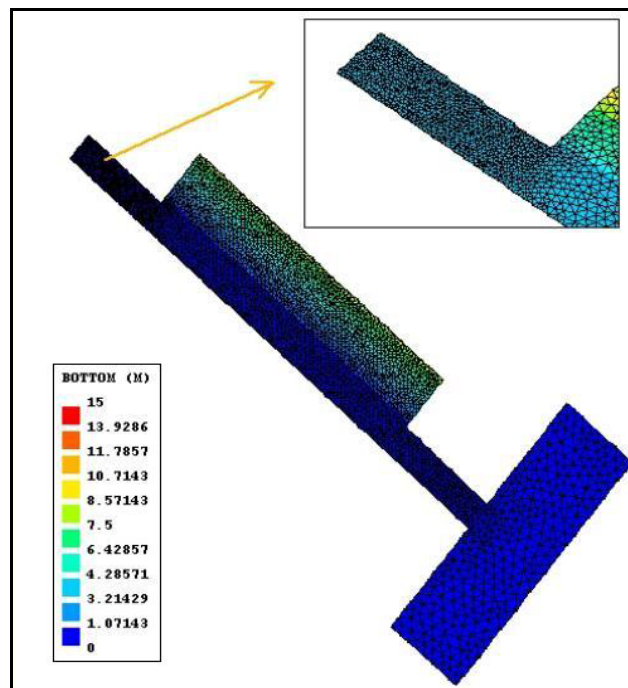


Figure 5-9: Domain of Model 3

The model results in Figure 5-10 represent clearly the wet and dry events that have been occurred periodically at the tidal flats in function of the tidal state. The bed is wet at high tide and dries out at low tide. Moreover, the circulation pattern at the tidal flats is also well simulated in the domain showing a good performance of the model.

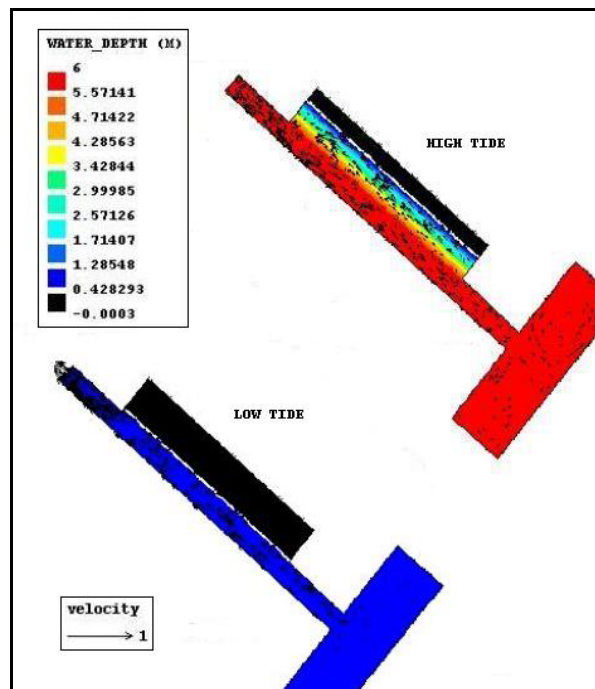


Figure 5-10: Model Results - Velocity Distribution in the Canal

The results obtained along the ideal modelling cases, give the certainty that the different parameter settings and the options chosen to represent every new complexity in the domain are correct. Therefore as a next step, the real domain will be implemented keeping the settings found before as a first approach to model the IJzer estuary hydrodynamics.

#### 5.4 2D Hydrodynamic Simulation of the IJzer Estuary

One of the major objectives of the present work is the hydrodynamic modelling of the IJzer estuary. After learning TELEMAC-2D software and testing the modelling approach in theoretical cases, a regular domain with the previous imposed settings and the bathymetry of IJzer Mouth has been implemented into the model.

In order to validate the previous parameter settings for the modelling of the real domain, the previously developed ideal tide has been prescribed at the open boundary side. The final case study has been developed after this with measured water levels (March 17<sup>th</sup> to 19<sup>th</sup>, 2003) recorded at the mouth of IJzer to set up the model of 'De IJzermonding' under real conditions. A Special attention has been given to inter tidal zones where sedimentation and erosion

processes might take place. In this way the basis for the development of a sediment transport model in the area are set in this study.

#### 5.4.1 Model Geometry

A lock gate is located at the upstream of the study area (Figure 5-11). This system regulates the water interchange between the North Sea and the IJzer River; therefore it is used to control the flood and saline water intrusion in the flat areas. The system is always considered as locked in the model domain, neglecting the effect of gate operation. Under this condition the hydrodynamics of the IJzer estuary are basically driven by tides; therefore density-stratification is not present in the estuary.

*Caluwaerts* (2003) used TELEMAC-2D to model the hydrodynamics of different ideal domains as a first approach to model the IJzer estuary. Within the model assumptions, the upstream part of the IJzer mouth as well as wet areas not included in the domain has been modelled by a rectangular reservoir.

Based on *Caluwaerts* analysis (2003), two dummy reservoirs of different size have been placed in the upstream part of the domain, balancing the water volume in the system. The biggest reservoir replaces the water volume at the upstream of inter tidal zones up to lock system (closed boundary). Another reservoir with the capacity of one third of the water volume modelled at the upper part of the estuary has been located on the left bank to represent an existing natural harbour, as it can be seen in Figure 5-12. These reservoirs have been included in the model domain for the purpose of elimination of the lock gate and existing small harbour. These could have also serve as the calibrating the model by resizing. The change of volumes of the reservoirs would allow the change of flow through the IJzer Mouth, thus providing an option to calibrate according to the observed velocity.

Bathymetry and DEM information have been merged to define the elevation of the model area. All the information in the domain is referred to TAW, which is also the reference system of the tidal sign imposed at the mouth. The final domain contains the canal and the neighbouring inter tidal zone (over the right bank).

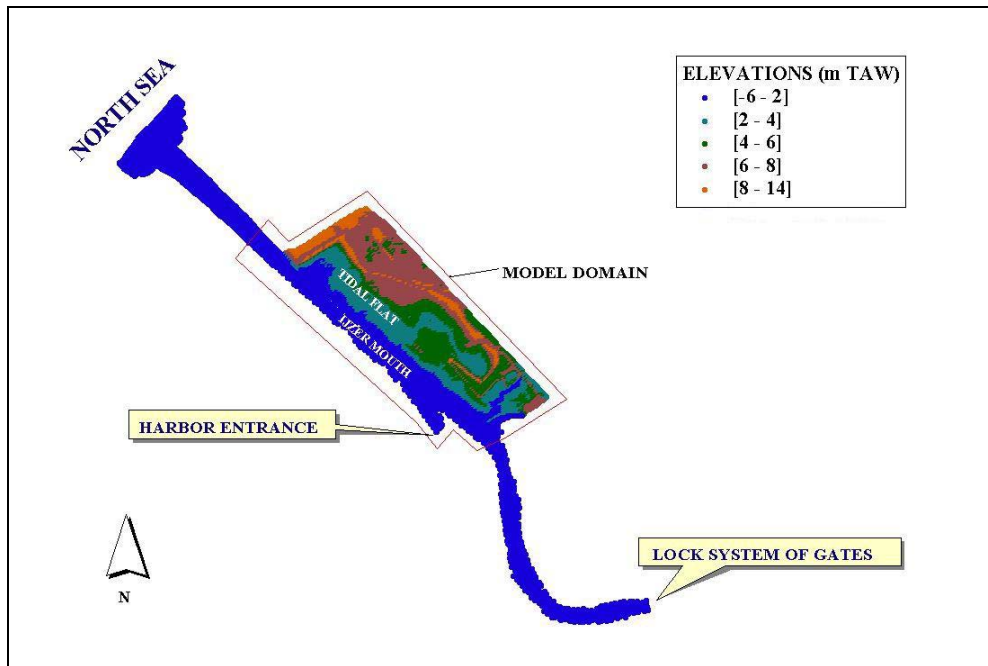


Figure 5-11: The IJzer Estuary

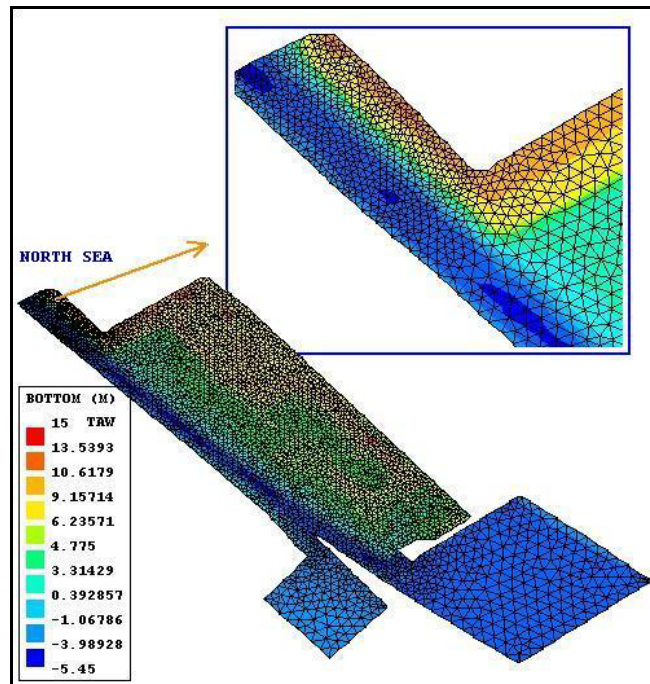


Figure 5-12: The IJzer Model Grid

### 5.4.2 Mesh Generation

Some missing values in the bathymetry of the mouth have been calculated using the Triangulated Irregular Network (TIN) interpolation method available at the Arc View environment. After the interpolation the elevation data have been imported into MATISSE for the mesh generation.

The grid resolution has been set at 20m for most of the domain. The resolution at the reservoirs and at the area near the canal mouth has been set in function of the required detail. For the area near the canal mouth a grid resolution of 10m was chosen in order to have more points at the open boundary; while for the reservoirs a grid resolution of 50m was chosen to avoid higher computation time.

### 5.4.3 Initial and Boundary Conditions

The water level in the domain has been imposed at the open boundary. The model boundary has been extended at the right bank of the IJzer mouth to include the neighbouring DEM. A liquid boundary file containing the tide information is read by the program (Figure 5-13). The initial water level in the domain is set the same as the water level imposed at the open boundary. For the ideal tide sign imposed, the initial water level at the domain is imposed at 3.5 m TAW as it was done for the ideal geometries. For a real tide sign registered at the open boundary a value of 4.10 m TAW is prescribed as the initial water level in the domain.

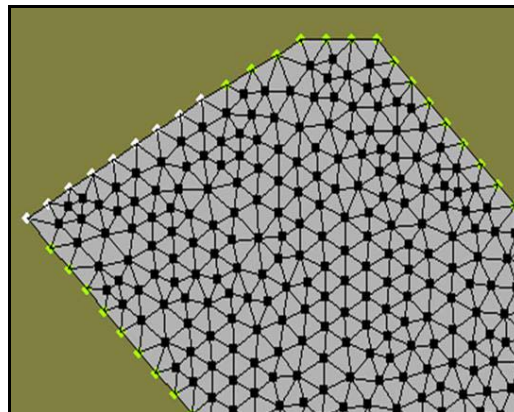


**Figure 5-13: Boundary Definition in the Real Domain. The White Points Represents the Open Boundary, while the Green Points are the Closed Boundary of the IJzermonding Domain.**

The Chezy's Law has been chosen once more to model the bottom friction for the IJzer domain. Three different friction coefficient values have been used for the modelling of the real domain: 60, 65 and 70  $\text{m}^{1/2} \text{s}^{-1}$ , varying the value used for the ideal geometries (65  $\text{m}^{1/2}\text{s}^{-1}$ ) to evaluate its influence in the model velocities for a non regular bottom elevation of the domain. An analysis of the results is discussed in *Chapter 6*.

#### **5.4.4 Tidal Flats**

The free surface gradient correction is applied for the treatment of the tidal flats during the modelling of the real domain with an ideal tidal signal imposed at the liquid boundary. As a further step, observed water levels have been imposed, and both methods, the free surface gradient correction and masking of exposed elements technique, have been applied for the treatment of the submerged/exposed areas, being the results from these different choices analysed in *Chapter 6*.

#### **5.4.5 Numerical Options**

Two scenarios for the hydrodynamics of the IJzer estuary have been modelled, one prescribing an ideal tidal sign at the canal mouth (the amplitude of 5m and a period of 12.42 hours) and the other with the observed tidal water level in TAW datum obtained from March 17 to September 19, 2003.

The time step for the computation has been set at 3 seconds for scenarios, fulfilling the Courant number criterion and accounting for feasible computation time. The simulation has been run for 3 days, with 25,920 time steps. The graphic and listing printout periods of the horizontal components of the velocity (U,V) and the water depth (H) are set every half an hour (1,800 sec).

#### **5.4.6 Model Outputs**

The IJzer model results have been printed out in Rubens during the last two-day simulations, skipping in this way the transition period during the first day. A FORTRAN routine to convert serafin format into an ASCII format has been used in order to obtain the model velocities in a



structural format, being able to compare them with available velocity measurements at the IJzer Mouth (March 19<sup>th</sup>, 2003).

## 5.5 The IJzer Model Performance

The 2D-hydrodynamic model of the IJzer estuary developed in the present work simulates the depth averaged north and east velocity components at each node within the domain. Based on the availability of field velocity measurements the model performance has been evaluated through a comparison process.

Three dimensional velocity data have been recorded by an Acoustic Doppler Current Profile (ADCP) at different points in the IJzer canal, from a nine hours field campaign on March 19th, 2003. The measurements have been covered for a complete ebb period and part of the rising tide. In order to evaluate the goodness of fit of the model, depth averaged velocity measurements at the IJzer estuary are required in time scale.

A MATLAB script developed by *Caluwaerts* (2003) to read and calculate the depth averaged velocity for every observed velocity-point (ADCP) has been modified in the present work. The routine gives an output of the date and the time of the records and the magnitude and direction of velocity. The Trapezoidal rule has replaced the previous formulation to compute the depth-averaged velocity to consider the logarithmic velocity distribution in the profile encountered in flow along a wall (*Graf*, 1998).

TELEMAC result file has been converted to an ASCII format, and a new routine, MVSRSV, has been developed in MATLAB to structure the simulated data in a matrix form. The MATLAB routine (MVSRCV), which reads the model result file, compares the model and the observed velocities at different cross and longitudinal sections in the estuary along the period of measurements. It compares the direction and magnitude of the observed velocity at every canal point along a cross or a longitudinal section, within the simulated velocity at the closest model point for the corresponding time step. The observed velocities have been separated at every thirty minutes and stored in different text files. Thus, the measurements recorded every half an hour can be compared with the corresponding model velocity output at the end of that period, as the printing out of TELEMAC-2D results has been set as the same time. The user

can define the model time step (print out time step) corresponding to the measurement period analysed as an input variable to the script.

Three types of plots are generated from this routine: “Model and Observed velocity magnitudes along a section”, “Observed vs. Model velocity magnitude” and “Observed vs. Model velocity direction”. The Root Mean Square Error (RMSE) value has been added for the scatter plots to measure distribution of the residuals with respect to the mean.

Each model point has more than one corresponding observed value as the observed number of points for velocity is higher than the model output at every section that have been analysed. In order to eliminate this problem and establish a clear comparison, the observed velocities have been averaged for the analysis. Thus, the scatter plots show the mean observed velocity, magnitude and direction, vs. the model output. The standard deviation of the averaged values is displayed with the mean in the velocity magnitude scatter plot, but it has been omitted in the case of velocity direction due to the proximity of the mean velocity direction values. Through out this process the performance of the model can be evaluated as a good approximation of the reality.

## Chapter 6: The IJzer Model Study Results

### 6.1 Introduction

The case study of 'De IJzermonding' is based on TELEMAC-2D modelling predictions for three days of simulation period. This period represents the spring tide condition for the observed water level in the simulation. The procedure of model set up and the results of the theoretical cases of IJzer estuary have been described in the previous chapter. The results of real cases using bathymetry of the channel with ideal and observed tide are incorporated in this chapter. The comparison of the model outputs with the real conditions are also shown in this chapter.

### 6.2 Flooding and Drying Event Ideal Tide

'De IJzermonding' is subject to flooding and drying process due to surface water elevation changes in the North Sea. This phenomenon is demonstrated in the Figure 6-1, where the spatial variation of water depths is indicated for the case of real bathymetry and ideal tidal signal. The model responds well for the variation of imposed water level at the open boundary. The water depth in the middle of the canal increases up to 11.4 m during the flooding event of ideal tide. The neighbouring tidal flat is also inundated and the water depth varies according to DEM. The relatively high terrain of the tidal flat dries out during the ebb phase. The water depth in the tidal flat is 0.4 m at some places during the ebb and maximum is 4.2 m at the middle of the IJzer mouth (Figure 6-1). Most of the places of the tidal flat are exposed to the atmosphere during ebb tide; thereby the vegetation and benthic materials are highly productive due to more oxygen supply and light.

Figure 6-2 shows the flow velocity vectors in the IJzer mouth along with inter tidal zone. The velocity also follows the direction of flooding and ebbing events. The average velocity of the IJzer River is 0.25 m/s in the middle and decreases along the bank. It is relatively high (1.2

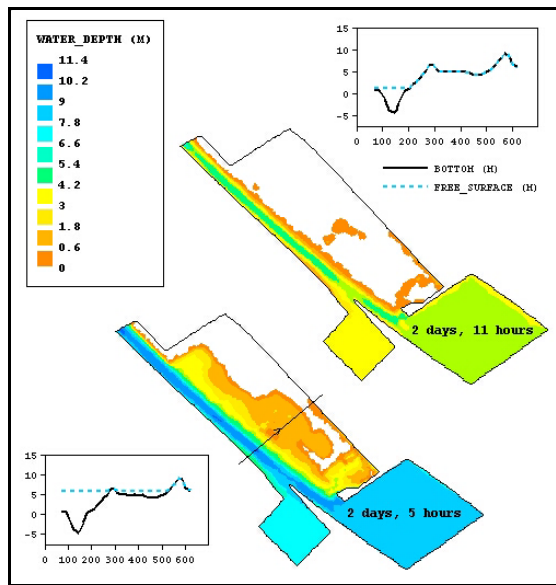


Figure 6-1: Water Depth at Rising & Ebb Tide

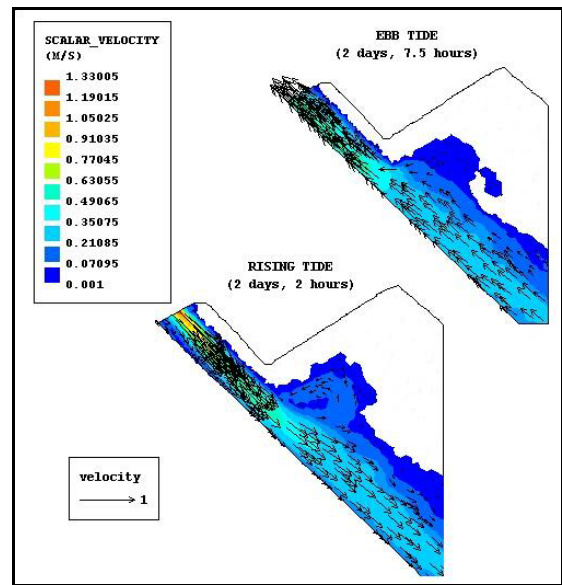


Figure 6-2: Velocity at Rising & Ebb Tide

m/s) at the entrance of the estuary. This might be due to the amount of water that needs to enter in the domain during flooding. It could also be influenced by the orientation of the model domain which has been explained in *Chapter 5* through a theoretical case study. The flow velocity in the tidal flat is very low, but it follows the variation of the tidal wave.

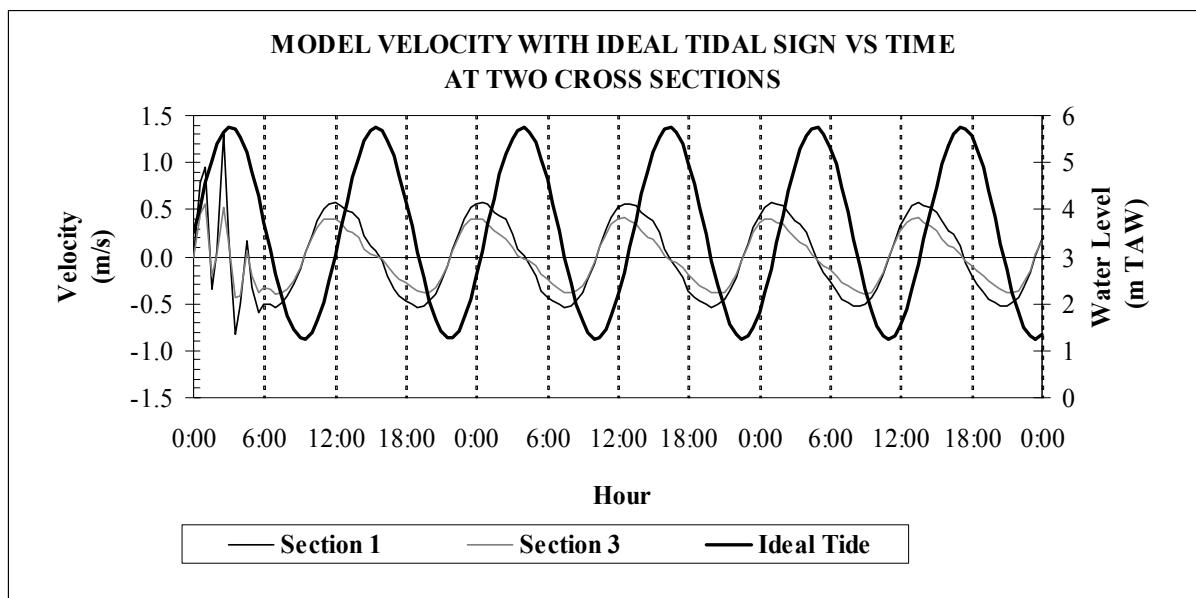


Figure 6-3: Time Series of Model Velocity Outputs at Different Section in the Middle of IJzermunding

The time series of model velocities for the simulation period of three days have been shown in the Figure 6-3 at a particular point in the middle of the IJzer mouth. The transition period is almost six hours at the beginning of the simulation time and after that period the model becomes numerically stable. The velocity peaks are obtained during the changing period of the flood and ebb current. Figure 6-3 represents the natural phenomenon of high velocities after the slack period. This model set up with ideal tide follows the natural events, which is the basis of further analysis with observed water level at the open boundary. The flooding and drying events make the verification of reasonable model parameters, which is kept as the same for the rest of the study.

### **6.3 Case Study with Observed Tidal Data**

A real domain influenced by an observed tidal signal has been set up for the case study of 'De IJzermonding'. The neighbouring inter tidal zone can be simulated using two different options defined by 'OPTIONS FOR THE TREATMENT OF TIDAL FLATS' keyword at the steering file. The name of the first option is 'Correction of Gradient of the Free Surface' and the second option is 'Masking of Exposed Elements'.

Figure 6-4 shows that the first option floods a considerable area of inter tidal zone, while some parts remain dry when the second option is applied. The second option, masking of the exposed element, considers the cells that are wet only at beginning of the computation. Once the dry cells are masked, they would not be involved in the computation anymore even if a higher water level is imposed at the open boundary.

This hypothesis has been verified by another scenario study with two different initial water levels in the second option. Figure 6-5 shows that a different number of masked elements are obtained from this analysis based on the initial imposed water level. At first, the model is simulated with the highest observed water level of 4.99 m TAW as the initial condition. The wet area obtained from this scenario is the same as the results obtained from the correction of free surface gradient. When the initial water level of 4.11 m TAW is imposed, a smaller area is wetted during the simulation.

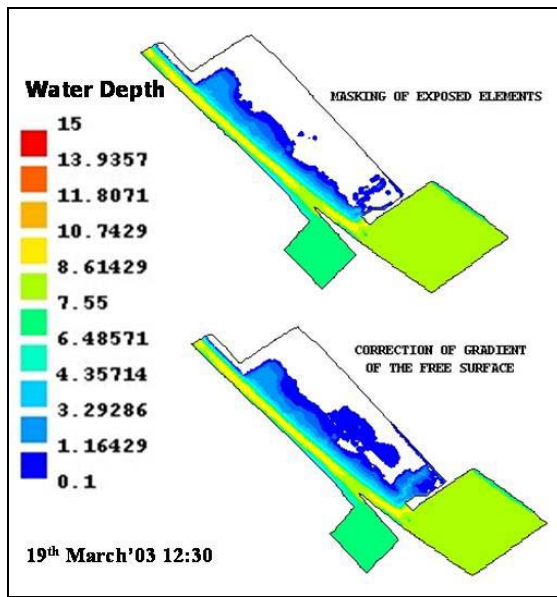


Figure 6-4: Comparison of two Options of Tidal Flats

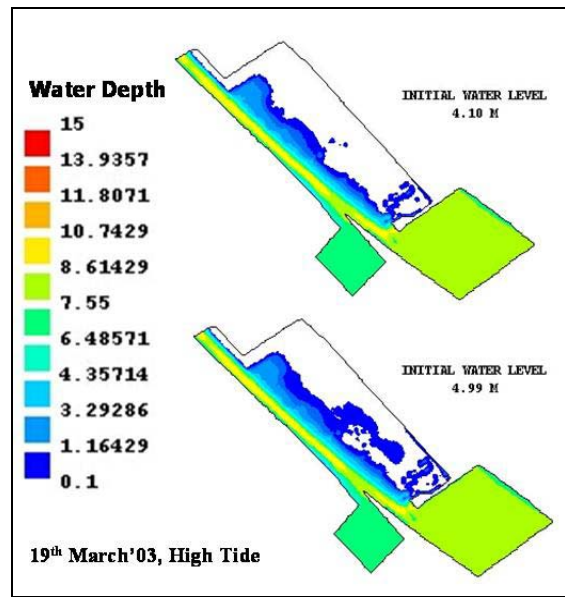


Figure 6-5: Masking Tidal Option with Different Initial Level

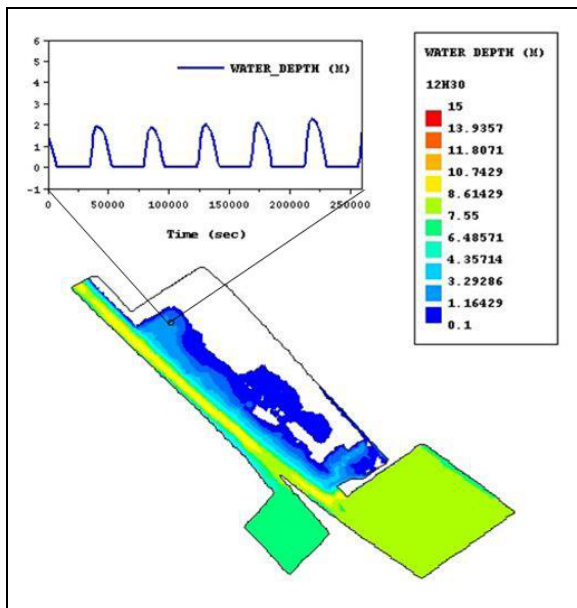


Figure 6-6: Water Depth and Flooding & Drying Event for the Observed Water Level

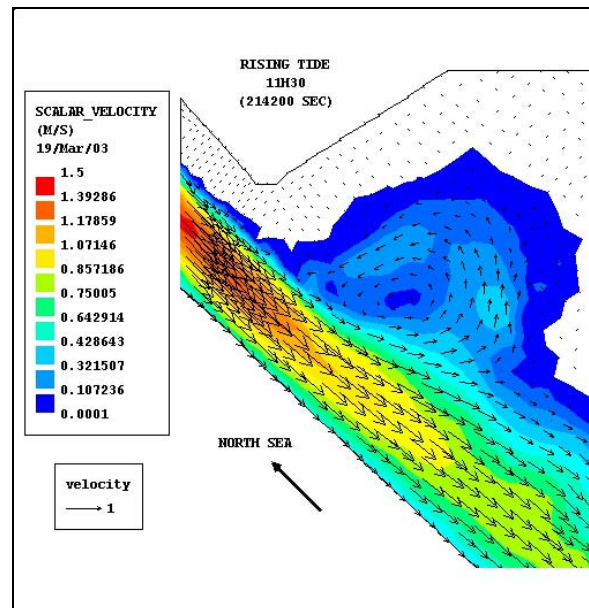
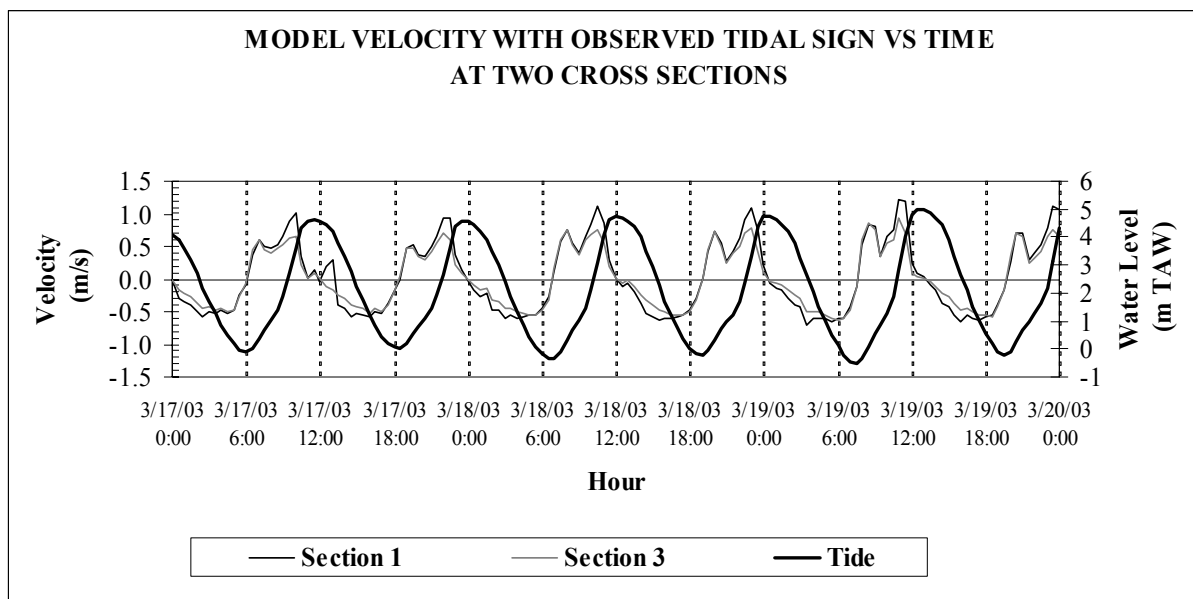


Figure 6-7: Velocity Recirculation at the Inter Tidal Zone during the Rising Tide

In this study the simulation period starts before the spring tide and the maximum water level is observed after three days. This limits the application of the masking of the dry elements option for the treatment of the tidal flats as the imposed initial water level is lower than the

peak at spring tide. In the other hand, the first option, which corrects the free surface elevation between dry and wet cells, carries out the computation in all the elements of the domain. Therefore, the first option for the treatment of tidal flat has been chosen for the rest of the analysis to provide more realistic outputs from TELEMAC-2D.

In Figure 6-6, one point in inter tidal zone is chosen for the temporal visualisation of water level. This point becomes dry during the ebb tide, shown by the zero water depth, while the water depth reached up to 2m during the flood tide. The time series of water depth in the tidal flat indicates the proper functioning of the final model with the observed tide prescribed in the open boundary. Figure 6-7 shows the incoming of velocity in IJzer estuary during the flood tide. It enters at a higher rate (1.5 m/s) in the mouth and is distributed along the width in tidal flat. A recirculation of the velocity is observed at inter tidal zone. The range of the velocity in the tidal flat varies between 0.1 and 0.4 m/s depending upon the depth.



**Figure 6-8: Time Series of Model Velocity at the Middle of the IJzer Mouth**

Figure 6-8 shows the time series of the model velocity at the middle of the sections and the observed tide during the simulation period. Two velocity peaks appear during the rising tide through out the whole period of simulation. It can be noticed that the change of water level is slower at the beginning of the rising phase and increased at higher rate up to the peak of high tide. This natural inertial behaviour of the system might affect the velocity pattern.

In the other hand, DEM of the tidal flat might also influence the unexpected velocity peaks shown in Figure 6-8. The IJzer estuary along with inter tidal mudflat are flooded when the water elevation rises up to its maximum value. The velocity increases according to the rise of water level in the study area. Considering the continuity of flow in the system, the velocity decreases after the first peak, when a considerable part of the tidal flat is inundated. It provides more area for water entering into the system with the correspondent drop in velocity. Consequently, more inflow of water would generate the second peak of velocity in the time series.

Other reasons influencing this unexpected behaviour of the velocity could be the combined effects of numerical solution scheme and the assumptions considered in the model. In order to reject the hypothesis of numerical instability, the model has been simulated for a time step as short as one second, which has not improved the situation. The assumptions related to the reservoir could also be the reason for this behaviour.

Once the model is set up, it has been tested with different Chezy's coefficients. Three trials have been performed with the coefficient values of 60, 65 and 70  $\text{m}^{1/2}\text{s}^{-1}$  to check the performance of the model at different scenarios. The velocity output obtained from this analysis is stated in the Figure 6-9. It can be demonstrated from the figure that there is no significant affect of Chezy's coefficient on the model results. The domain of the model is relatively small, thus the variation of the coefficient has negligible impact on the velocities inside channel. The Chezy's coefficient for IJzer estuary has been estimated as 65  $\text{m}^{1/2}\text{s}^{-1}$  after the trials.

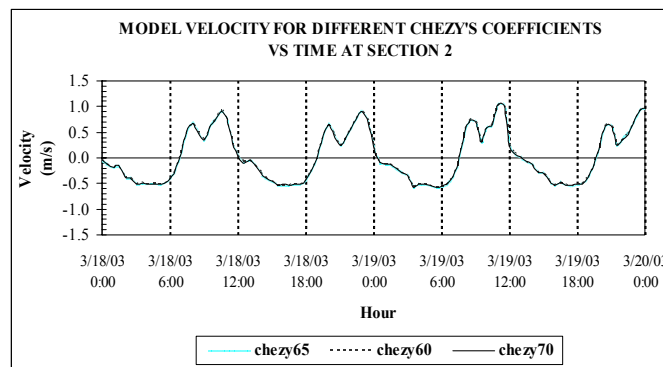


Figure 6-9: Comparison of Model Velocity with Different Chezy's Coefficient



## 6.4 Performance of the Model

Sectional and scatter plots have been generated from the comparison of the model velocity results within data collected at the IJzer estuary during the field campaign on March 19<sup>th</sup> 2003 (see Appendix D). Table 6-1 shows the root mean square error and the goodness of fit of the model velocity during the Ebb and the Rising phase of the observed tidal period. From those results it can be noticed that the model velocity magnitudes follow the observed natural pattern better during ebb tide than during the rising phase. Due to this, the overall performance of the model has been decreased to 0.48.

**Table 6-1: Performance of the model velocity magnitudes along Tide**

<b>Tidal Phase</b>	<b>Mean Velocity Observed (m/s)</b>	<b>Mean Velocity Model (m/s)</b>	<b>RMSE (m/s)</b>	<b>GOF</b>
<b>Ebb Tide</b>	0.2676	0.2636	0.0978	0.81
<b>Rising Tide</b>	0.2435	0.3553	0.2515	0.02
<b>Overall</b>	0.2590	0.2960	0.1689	0.48

The longitudinal plots shown in Figure 6-10 indicate that the model velocity magnitudes follow the spatial pattern observed at the channel during the last period of the ebb phase and at slack (19h30). However, under and overestimations are observed in the longitudinal section plots during rising tide. The model velocities near the channel mouth are increased and the observed values are overestimate after 19:30 during the change of tidal phases. The matching of model and observed velocity is obtained for few compared points along the channel at 21:00. This effect is also recorded in some transversal section plots during the rising phase, which is shown in Appendix D.

The temporal plots shown in Figure 6-11 could better explain this apparently strange behaviour of the model velocity observed in the sectional plots. It can be noticed that the double peaks observed in the model velocity pattern during rising tide is printed out in the spatial scale plots as well. The temporal scale plots show that observed magnitudes close to the model velocities are recorded at section 1 and 2 during the rising tide. At section 1, the last observed magnitude is close to the model velocity; while the same situation is observed at section 2, where the first model velocity peak is reported by the natural system.

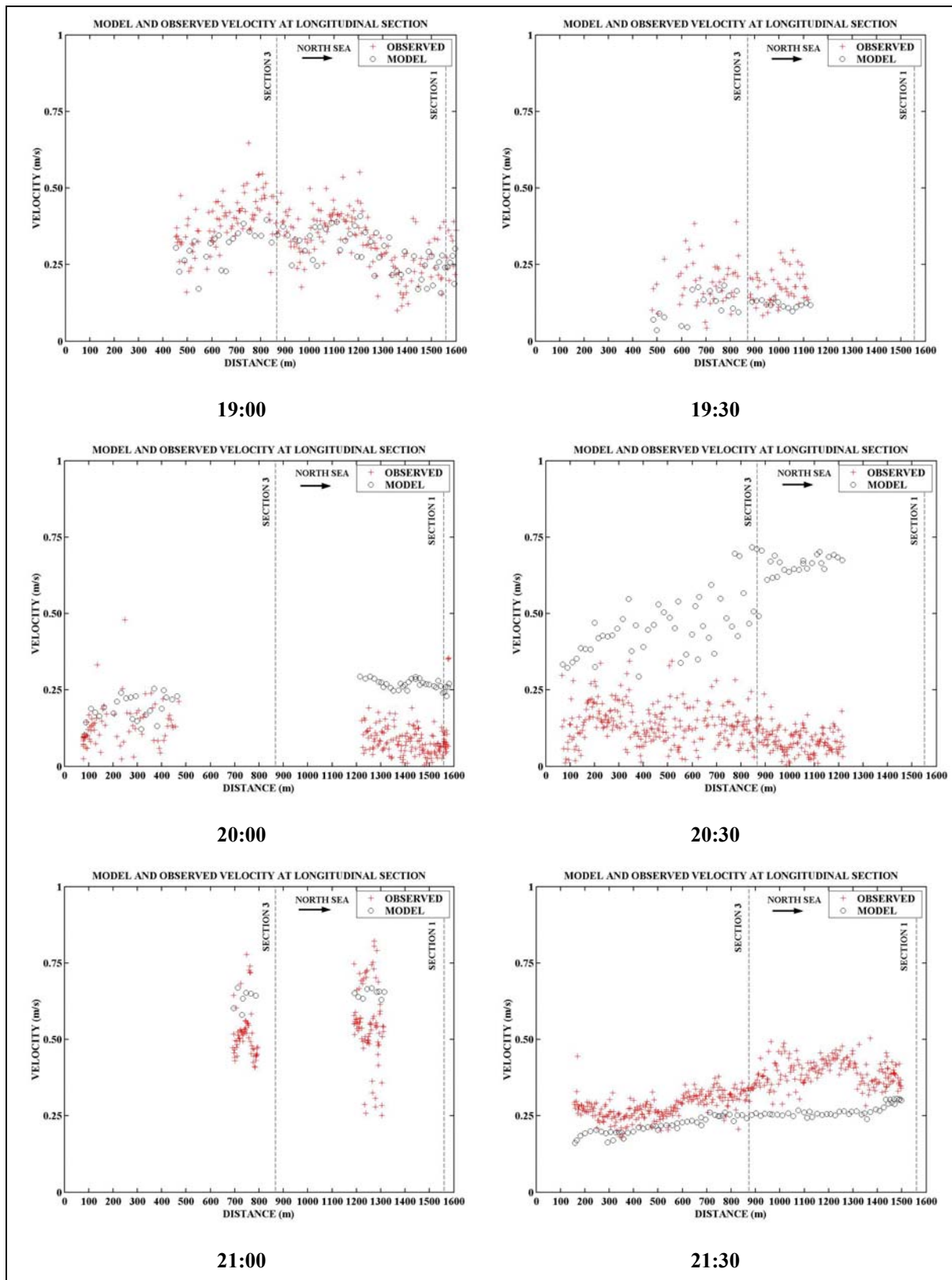


Figure 6-10: Longitudinal Sections at the IJzer Estuary with Observed and Model Velocity along Part of the Ebb and Rising Phase for the Tidal Period on March 19<sup>th</sup> 2003

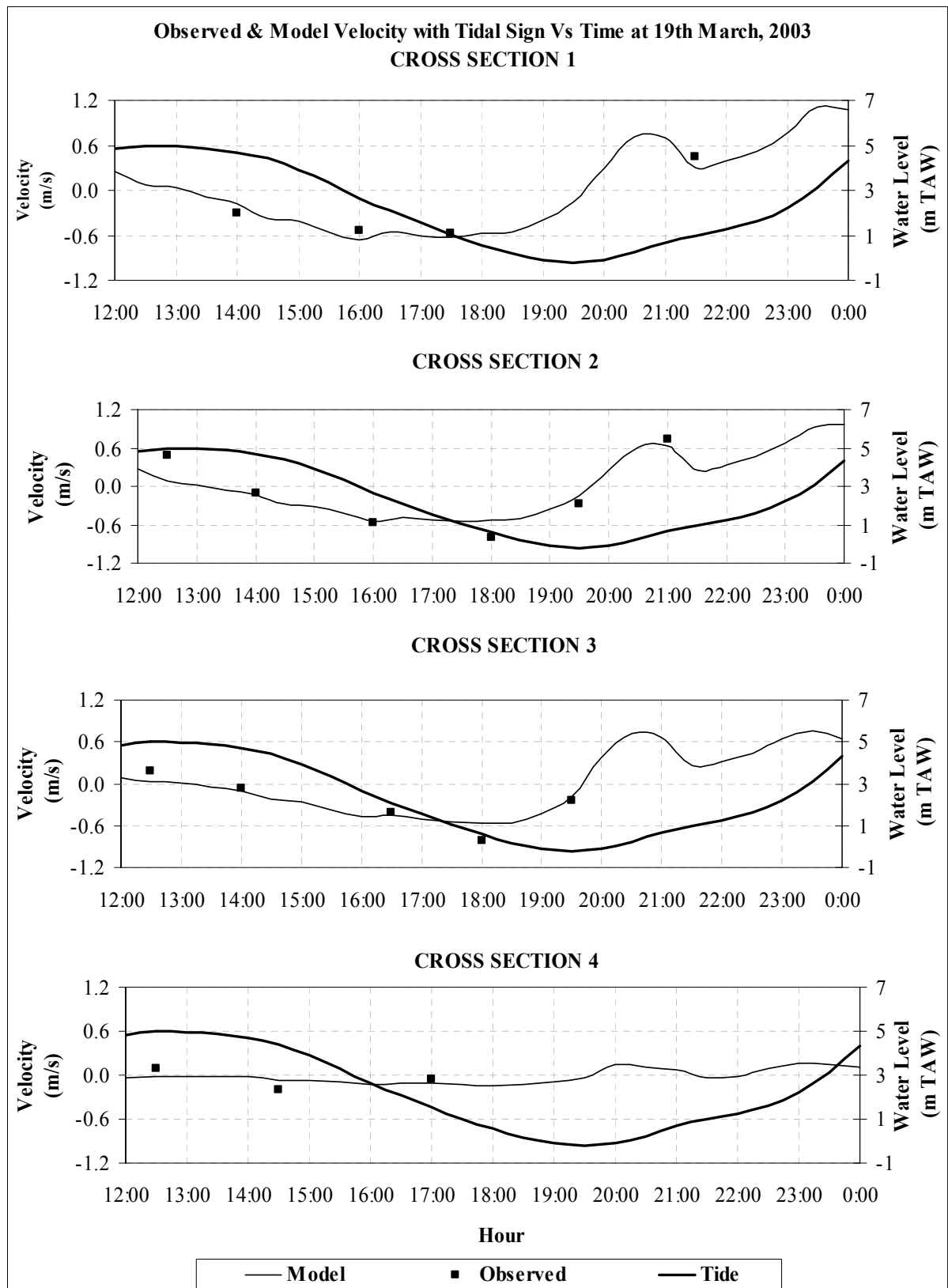


Figure 6-11: Comparison of Model Velocity with Observed Data in Temporal Scale

Sections 3 and 4 do not record enough information during rising tide to contribute with this analysis. However, a good performance of the model can be appreciated from these sections. Table 6-2 shows the model performance for the velocity comparison at different sections in the canal during ebb and rising tidal phases. The RMSE values calculated for every section along the canal show that the model velocity fits well for the observed velocities at section 1 and 4 as well as for the longitudinal section recorded during Ebb tide. The other sections provide higher RMSE, but the mean observed and model velocities are close enough to be reasonable. The RMSE observed during rising tide is high for all the sections analysed.

**Table 6-2: Performance of the 2-D Hydrodynamic model along the transversal sections at different tidal phases**

<i>Cross Sections</i>		<b>Mean Velocity Observed (m/s)</b>	<b>Mean Velocity Model (m/s)</b>	<b>RMSE (m/s)</b>
<b>Ebb Tide</b>	<b>Section 1</b>	0.4299	0.4729	0.0936
	<b>Section 2</b>	0.2592	0.2160	0.1557
	<b>Section 3</b>	0.2460	0.2218	0.1263
	<b>Section 4</b>	0.0972	0.0817	0.0697
	<b>All Sections</b>	0.2808	0.2711	0.1220
<b>Rising Tide</b>	<b>All Sections</b>	0.4407	0.3988	0.1825
<b>Overall</b>		0.2986	0.2853	0.1301
<i>Longitudinal Sections</i>				
<b>Ebb Tide</b>		0.2619	0.2605	0.0855
<b>Rising Tide</b>		0.2290	0.3522	0.2558
<b>Overall</b>		0.2481	0.2990	0.1782

Figure 6-12 shows the velocity magnitude along the canal for a longitudinal transect and the velocity magnitude distribution along the transversal section 1 during ebb tide. It can be noticed that although the model velocity along the channel is close to the observed one, some overestimations occur toward the last part of the canal and on the left side of the section 1. This is dramatically increased during the rising period of the model as explained before. Nevertheless, the results are good in the sense that the differences in velocity magnitude between the model and the observed values are small between points that do not have the same position. Moreover, the performance of the model directions fits well for the whole period of measurements, except in the slack period where the natural system is very dynamic. The model velocity along the transversal section follows the natural parabolic pattern of the

observed velocities. Therefore, the errors calculated by the RMSE technique in the scatter plots for the velocity magnitude and direction in each case can be considered as acceptable.

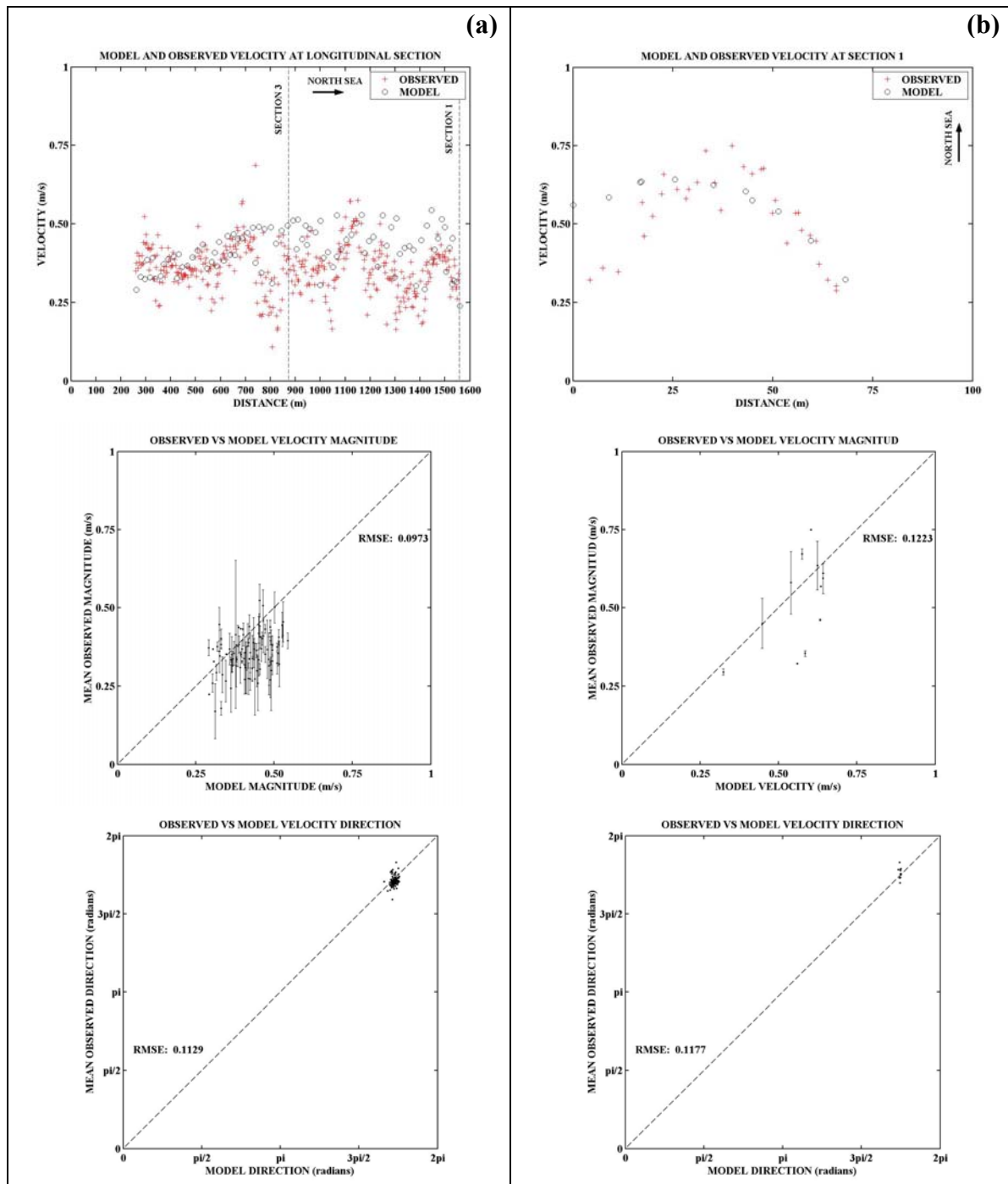


Figure 6-12: Plots of the Observed and Model Velocity at the IJzer Estuary on March 19<sup>th</sup> 2003 at 17:30 (Ebb Phase): (a) Longitudinal Section with Scatter Plots for Velocity Magnitude and Direction, (b) Transversal Section with Scatter Plots for Velocity Magnitude and Direction

As a last remark to be mentioned here is that the velocity direction pattern of the IJzer mouth, influenced by tides, is well simulated by the model velocity direction as it is shown in the scatter plots of velocity direction for all the sections along the whole period of measurements except during the slack time (See Appendix D).

## **6.5 Conclusion**

In the case study of '*De IJzermonding*', the comparison of the velocity shows reasonable output of magnitude and direction from the model, therefore the volume of the reservoir has not been changed in this study. The measurements are available up to 21:00 hours when the flooding event is not over. The raise of water level after the ADCP measurement leads to have another peak velocity in the model, which cannot be compared with real data. Moreover, the performance of the model directions fits well for the whole period of measurements, except in the slack period where the natural system is very dynamic. It can be concluded from the performance of the model and above discussions that the modelling approaches are well adapted for the simulation of the IJzer estuary hydrodynamics.

## Chapter 7: Conclusion and Recommendations

According to the main objective of this thesis research a two dimensional hydrodynamic model has been implemented for the IJzer estuary using TELEMAC-2D software. The model domain represents the study area with certain accuracy. The deviation of the model results from the nature may arise from the uncertainty in measurement and parameter estimation.

The bathymetry data used for the IJzermonding is taken from the survey conducted at July 2002 and the simulation period consists three days of March 2003. The dredging of the navigation channel at Nieuwpoort usually takes place at the beginning of each year. Due to this reason the model results can be differed slightly from the reality. Furthermore, the ADCP measurement of the velocity has also been performed after the dredging operation. Some weaknesses are observed in the velocity measurements at the beginning of the campaign. Missing data in the continuous velocity profile leads to exclude that vertical from the available data set. Also, the measurement of the campaign on 19<sup>th</sup> March, 2003 does not cover the full tidal cycle. It has been started at the beginning of ebb tide, but at the end of the rising tide the velocity measurements are not recorded. Therefore, the velocity pattern could not be compared during the peak flood tide. Moreover, the observed water level at the IJzer mouth might also cause the measurement error in the study.

The uncertainty due to parameter estimation might be occurred during choosing the Chezy's and viscosity coefficients in the model. Different values of Chezy's coefficients have been tested during the research process to minimise this uncertainty. It has been mentioned in *Chapter Six* that small changes in the Chezy's coefficient value has negligible effect on the velocity magnitudes in this study area as the length of IJzer channel is relatively small. The viscosity coefficient is set in the keyword of the steering file according to the suggestion provided in the TELEMAC-2D Users Manual. Further research on the parameter estimation could be performed to check the sensitivity of the model.

A limitation for the treatment of the tidal flats at the IJzer estuary has been discovered for this particular study in the masking process during the computation. The exposed elements detected as dry at the beginning of the simulation are masked and the process is not updated along the simulation. This method is limited for hydrodynamic simulations with an initial high water level prescribed into the domain which is useful for some other engineering applications of risk assessments.

The numerical results presented in *Chapter Six* have shown that the model is reliable to simulate flooding and drying events and generating velocities at inter tidal zones. Therefore, further research work in erosion and sedimentation processes occurring in 'De IJzermonding' can be performed based on the first approach reached by the model. Nevertheless, the behaviour of model velocity during rising tide has also been discussed in *Chapter Six*. The reasoning behind the double peaks of the model velocity could be justified in a future research work.

As it has been shown in the results, the magnitudes and directions of the model velocity at the navigation canal fit well with the observed values during the Ebb phase. Additionally, the natural pattern of the velocity field influenced by tides is well demonstrated when the change in tide phase occurs as well as the parabolic velocity distribution in the cross section. In the other hand, the double peaks of the model velocity during the rising phase show a deviation from the measurements in the sectional profiles. The temporal variability of the observed velocity for a position in the canal is well followed by the model velocity even during rising tide. Therefore, further research along with field campaign is needed for the simulation of the velocity magnitude during the rising tidal period.

Variations in the water volume of the domain can be included as well as deeper analysis of the coordinate system limitations in the software, which is demonstrated by the ideal model of a symmetric canal. In the other hand more observed velocity data are required to know in detail to evaluate the natural behaviour of the system and thereby establish a better criterion of model performances.

Some features of the domain that have not been covered in the present modelling work could be implemented in a further research to account for a more realistic and accurate



hydrodynamic model. The physical and model boundary at the right bank of the IJzer mouth is not the same in this study. This model geometry could be updated in a more realistic way by adding the existing wall at the right bank near inter tidal zone. The updated bathymetry data of the navigation channel should be implemented into the model geometry definition to consider the recent changes in the bottom elevation of the domain due to annual dredging works.

In order to evaluate better the model performance, comparisons of the model velocities with observed values should cover at least one tidal cycle to evaluate with certainty the goodness of fit of the hydrodynamic simulation. It is also recommended to have more measurements covering some conjugative days in spring and neap tides. The adequate data are the only basis to calibrate and validate the model. On the contrary, it is advised to change the model printout period from thirty minutes to fifteen minutes to compare the observed velocities with model outputs for a time step coinciding with the middle of the time interval of the measurements. This would certainly improve the comparison results between the observed and model velocity in the future research.

## References

- Adam, S. (2004). Characterization of Intertidal Mudflats using Hyperspectral Remote Sensing. Case Study: 'De IJzermonding'. *Thesis Dissertation, Department of Earth Observation, Katholieke Universiteit Leuven.*
- Allen, J.R.L. (2000). Morphodynamics of Holocene saltmarshes: a review sketch from the Atlantic and Southern North Sea coasts of Europe. *Quaternary Science Reviews* 19, 1155–1231.
- Bates, P.D., Anderson, M.G., Hervouet, J.M., Hawkes, J.C. (1997). Investigating the behaviour of two-dimensional finite element models of compound channel flow. *Earth Surface Processes and Landforms* 22, 3–17.
- Bates, P.D., Horrit, M., Hervouet, J.M. (1998). Investigating two-dimensional, finite element predictions of floodplain inundation using fractal generated topography. *Hydrological Processes* 12, 1257–1277.
- Boussinesq, J. (1903). *Theorie Analytique de la Chaleur. Gauthier-Villars, 2*
- Brookes, A.N., Hughes, T.J.R. (1982). Streamline Upwind/Petrov–Galerkin formulations for convection dominated flows with particular emphasis on the incompressible Navier–Stokes equations. *Computer Methods in Applied Mechanics and Engineering* 32, 199–259.
- Carmo, J.S.A. and Santos, F.J.S. (2002). Near-shore sediment dynamics computation under the combined effects of waves and currents. *Advances in Engineering Software, Volume 33, Issue 1, January 2002, Pages 37-48.*
- Caluwaerts, E. (2003). Studie van Hydrodynamica en Sediment Transport in de IJzermonding. *Thesis Dissertation, Department of Civil Engineering, Katholieke Universiteit Leuven.*
- Deboeuf, C. & Herrier, J.L. (2002). The restoration of mudflats, saltmarshes and dunes on the eastern bank of the Yzer-rivermouth, Nieuwpoort. In: *Littoral 2002, 6th International Symposium. A Multi-disciplinary Symposium on Coastal Zone Research,*, eds.Veloso-Gomes, F., Taveira-Pinto, F. & das Neves, L.Eurocoast & EUCC - The Coastal Union, 201-202.
- Fischer, N.I. (1993). *Statistics of Circular Data. Cambridge University Press, 151 pp.*
- Frame Project. <http://www.frameproject.org/demo/ijzermonding.htm>. *Date Accessed 2/8/04.*

- Fernandes, E.H.L., Dyer, K.R., Moller, O.O. and Niencheski, L.F.H. (2002). The Patos Lagoon hydrodynamics during an El Niño event (1998). *Continental Shelf Research, Volume 22, Issues 11-13, July-August 2002*, Pages 1699-1713
- Hervouet, J.M., Van Haren, L. (1994). TELEMAC-2D Principal Note. Electricite de France Rapport HE-43/94/051/B.
- Galland, J.C., Goutal, N., Hervouet, J.M. (1991). TELEMAC: a new numerical model for solving shallow water equations. *Advances in Water Resources 14*, 138–148.
- Giardino, A. (2003). Tidal Simulation using TELEMEC2D and HN2D Models. *Thesis Dissertation, Facolta di Ingegneria. Politecnico Di Torino*.
- Graf, W.H. (1998). Fluvial Hydraulics. Flow and Transport Processes in Channels of Simple Geometry. *John Wiley and Sons Ltd. Publishers, UK*. Page 10.
- Ji, Z.G., Morton, M.R. and Hamrick, J. M. (2001). Wetting and Drying Simulation of Estuarine Processes. *Estuarine, Coastal and Shelf Science, Volume 53, Issue 5, November 2001*, Pages 683-700
- Lohrer, A.M. and Wetz, J.J. (2003). Dredging-induced nutrient release from sediments to the water column in a southeastern saltmarsh tidal creek. *Marine Pollution Bulletin, Volume 46, Issue 9, September 2003*, Pages 1156-1163
- Luo, W. (1995) Wind Wave Modeling in Shallow Water. *Doctoraatsthesis, Departement Burgerlijke Bouwkunde K.U.Leuven*.
- Malcherek, A. (1999). Applications of TELEMAC-2D in a narrow estuarine tributary. *The TELEMAC Modelling System, Hydrological Processes, Volume 14, Issue 13*. Pages 2293 – 2300.
- Marchuk, G.I. (1975). *Methods of Numerical Mathematics*, Springer, Berlin, 316pp.
- Mardia, K.V. (1972). *Statistics of Directional Data. Probability and Mathematical Statistics. A series of monographs and textbooks. Academic Press Inc. (London) Ltd*. Pages 21-28.
- Ministry of Flanders - Waterways and Maritime Affairs Administration (AWZ).  
<http://dup.esrin.esa.int/users/summaryu10.asp>
- Pugh, D.T. (1987). *Tides, Surges and Mean Sea-level. A handbook for engineers and scientists. John Wiley and Sons Ltd. Publishers, UK*. Pages 97-111
- Rycke, A.D., Devos, K., Sas, M., Decler, K. (2003). Towards natural flood reduction strategies. *In: Proceedings of International conference, Warsaw, 6-13 September 2003*.
- Soulsby, R.L. (1997). *Dynamic of Marine Sand. Thomas Telford (Ed.)*. London. 51pp.

Schneggenburger, C. (1998). Spectral Wave Modelling with Non-Linear Dissipation. *Report GKSS-Forschungszentrum Geesthacht GmbH, Appendix A.4.*

TELEMAC-2D Software, Version 5.2, User Manual (2002). EDF-DRD

TELEMAC-2D Software, Version 5.2, Reference Manual (2002). EDF-DRD

Wal, D. van der & Pye, K. (2004). Patterns, rates and possible causes of saltmarsh erosion in the Greater Thames area (UK). *Geomorphology*. <http://www.sciencedirect.com/>

Wetland Restoration, 2001. EPA fact sheet 843-F-01-002e  
[http://www.epa.gov/owow/wetlands/facts/restoration\\_pr.pdf](http://www.epa.gov/owow/wetlands/facts/restoration_pr.pdf)

## Table of Contents

<b>Acknowledgement</b> .....	<b>i</b>
<b>Abstract</b> .....	<b>ii</b>
<b>Table of Contents</b> .....	<b>iii</b>
<b>Table of Figures</b> .....	<b>v</b>
<b>Table of Tables</b> .....	<b>vi</b>
<b>List of Abbreviation</b> .....	<b>vii</b>
<b>Chapter 1: Introduction</b> .....	<b>1</b>
1.1 Overview .....	1
1.2 Objective of the study.....	2
1.3 Scope of the study .....	3
<b>Chapter 2: Characteristics of the Study Area</b> .....	<b>4</b>
2.1 Study Area .....	4
2.2 Flora and Fauna .....	5
2.3 Brief History of 'De IJzermonding' .....	6
2.4 Problem Description .....	7
<b>Chapter 3: Data Analysis</b> .....	<b>9</b>
3.1 Reference System .....	9
3.1.1 WGS84 and ED50 .....	9
3.1.2 UTM Projection.....	9
3.2 Bathymetry .....	10
3.2.1 Interpolation Method .....	11
3.2.2 Interpolation of Bathymetry .....	12
3.3 Tides .....	13
3.4 ADCP & CTD Measurement.....	14
<b>Chapter 4: TELEMAC-2D Software</b> .....	<b>16</b>
4.1 TELEMAC-2D System .....	16
4.2 2D Hydrodynamic Simulation in TELEMAC.....	17
4.2.1 Model Assumptions.....	17
4.2.2 Hydrodynamic Equations .....	18
4.3 Model Inputs.....	20
4.3.1 The Mesh Generation .....	20
4.3.2 Boundary Conditions.....	21
4.4 The Numerical Schemes.....	22
4.4.1 The Courant Number Management .....	23
4.4.2 The Turbulence Model .....	23
4.4.3 The Friction Law .....	23
4.5 Treatment of the Tidal Flats .....	24
4.6 Model Output.....	25
4.6.1 Rubens: the Graphical Postprocessor .....	25

<b>Chapter 5: Methodology of Hydrodynamic Modelling .....</b>	<b>26</b>
5.1 Introduction .....	26
5.2 General Model Settings .....	26
5.2.1 Geometry Definition.....	26
5.2.2 Initial Conditions .....	27
5.2.3 Boundary Conditions.....	27
5.2.4 The Friction Law .....	28
5.2.5 Numerical Options.....	28
5.3 2D-Hydrodynamic Model for Ideal Channels with an Ideal Tide Influence.....	29
5.3.1 Model 1: Rectangular Canal with a Reservoir.....	29
5.3.2 Model 2: Rectangular Channel with a Side Basin and a Reservoir.....	33
5.3.3 Model 3: Rectangular Canal Considering Tidal Flats and a Single Reservoir.....	35
5.4 2D Hydrodynamic Simulation of the IJzer Estuary.....	36
5.4.1 Model Geometry.....	37
5.4.2 Mesh Generation .....	39
5.4.3 Initial and Boundary Conditions .....	39
5.4.4 Tidal Flats.....	40
5.4.5 Numerical Options.....	40
5.4.6 Model Outputs .....	40
5.5 The IJzer Model Performance .....	41
<b>Chapter 6: The IJzer Model Study Results .....</b>	<b>43</b>
6.1 Introduction .....	43
6.2 Flooding and Drying Event Ideal Tide.....	43
6.3 Case Study with Observed Tidal Data.....	45
6.4 Performance of the Model .....	49
6.5 Conclusion.....	54
<b>Chapter 7: Conclusion and Recommendations .....</b>	<b>55</b>
<b>References.....</b>	<b>58</b>
<b>Appendix A Steering Files of Different Modelling Cases.....</b>	<b>61</b>
<b>Appendix B Raw Data Files.....</b>	<b>66</b>
<b>Appendix C MATLAB Scripts.....</b>	<b>69</b>
<b>Appendix D Graphical Analysis of Model Performance.....</b>	<b>78</b>
<b>Appendix E Mathematical Formulation of Statistical Analysis.....</b>	<b>96</b>

## Table of Figures

Figure 2-1: Study Area of 'De IJzermondig' .....	4
Figure 3-1: Relation between TAW and MLLWS Reference Systems at Nieuwpoort.....	11
Figure 3-2: Interpolation Results .....	12
Figure 3-3: Model Domain .....	13
Figure 3-4: Time Series of Tidal Cycle .....	14
Figure 3-5: Comparison of Flow Velocity at Different Sections of the IJzer Mouth Measured by ADCP .....	15
Figure 3-6: Processing of CTD Measurements with SEASAVE Software.....	15
Figure 4-1: 2D-Hydrodynamic Modelling in TELEMAC System.....	16
Figure 4-2: Free Surface Gradient Correction Method .....	24
Figure 5-1: Boundary Definition .....	27
Figure 5-2: Domain of Model 1 .....	30
Figure 5-3: Model Results - Velocity Components and Free Surface Elevation .....	31
Figure 5-4: Model Results - Velocity Distribution in the Channel .....	31
Figure 5-5: Model Results - Variations in the Orientation of the Model 1 .....	32
Figure 5-6: Model Results - Velocity Distribution of the North and the East Oriented Canals .....	33
Figure 5-7: Domain of Model 2.....	34
Figure 5-8: Model Results - Velocity Distribution at the Domain .....	34
Figure 5-9: Domain of Model 3 .....	35
Figure 5-10: Model Results - Velocity Distribution in the Canal .....	36
Figure 5-11: The IJzer Estuary .....	38
Figure 5-12: The IJzer Model Grid.....	38
Figure 5-13: Boundary Definition in the Real Domain. The White Points Represents the Open Boundary, while the Green Points are the Closed Boundary of the IJzermondig Domain.....	39
Figure 6-1: Water Depth at Rising & Ebb Tide.....	44
Figure 6-2: Velocity at Rising & Ebb Tide .....	44
Figure 6-3: Time Series of Model Velocity Outputs at Different Section in the Middle of IJzermondig .....	44
Figure 6-4: Comparison of two Options of Tidal Flats .....	46
Figure 6-5: Masking Tidal Option with Different Initial Level .....	46
Figure 6-6: Water Depth and Flooding & Drying Event for the Observed Water Level.....	46
Figure 6-7: Velocity Recirculation at the Inter Tidal Zone during the Rising Tide.....	46
Figure 6-8: Time Series of Model Velocity at the Middle of the IJzer Mouth.....	47
Figure 6-9: Comparison of Model Velocity with Different Chezy's Coefficient .....	48
Figure 6-10: Longitudinal Sections at the IJzer Estuary with Observed and Model Velocity along Part of the Ebb and Rising Phase for the Tidal Period on March 19 <sup>th</sup> 2003.....	50
Figure 6-11: Comparison of Model Velocity with Observed Data in Temporal Scale.....	51
Figure 6-12: Plots of the Observed and Model Velocity at the IJzer Estuary on March 19 <sup>th</sup> 2003 at 17:30 (Ebb Phase): (a) Longitudinal Section with Scatter Plots for Velocity Magnitude and Direction, (b) Transversal Section with Scatter Plots for Velocity Magnitude and Direction.....	53

## **ACKNOWLEDGEMENT**

This Master's dissertation has represented to us the cause of many difficulties but at the same time, and the thanks to the Lord, the source of many and by far pleasant achievements and sensations. Many people have contributed directly or indirectly to this very positive balance and as such, we would like to refer briefly as to some of them.

We would like to express our sincere gratitude and appreciation to the promoter Prof. Jaak Monbaliu. This work would not have been accomplished without his deep consideration and advice. His supervision, guidance and suggestions are landmark to support the entire work of this Master's Dissertation.

We are profoundly indebted to all the professors of IUPWARE for offering this course, which has certainly increased our background in Water Resources Engineering.

A special recognition is given to Alessio Giardino for his continuous support though out the whole research period. His technical skills about the TELEMAC software and sharing of knowledge have enabled us to work more efficiently.

The colleagues in the Hydraulic Laboratory, Esam, Jesus, Luis, Marc, Raul, Rosalia and Stefanie have always supported us sincerely for any help required during the study. They made us feel like another member of the research team. We have passed a very pleasant time during the coffee break and received moral and technical supports from them to accomplish this research.

Also, we would like to thank the Flemish Interuniversity Council (VLIR) of Belgium for granting scholarship for the whole study period of two years.

Finally, our eternal gratefulness and gratitude goes towards our parents for their love, moral support and continued encouragements during the two years of absence from the home.



## **ABSTRACT**

The restoration of degraded tidal wetlands is essential to ensure flood protection and water quality of environments that offer natural habitat for flora and fauna. Currently, The Flemish Government (AMINAL) is working at the restoration of an important coastal wetland at the IJzer estuary in Nieuwpoort: '*De IJzermonding*' natural reserve. The investigation of the hydrodynamic processes in IJzermonding is an important component of this restoration project, as well as for this research.

A numerical two dimensional hydrodynamic model using TELEMAC-2D has been set up for the IJzer estuary including the tidal flats of the neighbouring nature reserve. The flow velocity is identified as the most important model output variable to investigate sedimentation and erosion processes at the mudflats as it provides good indication of the bottom shear stress. Current velocities are also needed for further modelling of sediment transport processes. At first, a number of theoretical cases with different canal geometry and idealised tidal signal imposed at the canal mouth have been experimented to become familiar with the software and to establish the feasible model parameters. The real domain with the observed water level imposed at the liquid boundary has been implemented at the final step for the IJzermonding hydrodynamic modelling. GIS techniques are widely used for the pre-processing of model inputs and conversion of model data. The spatial and temporal performance of the model velocity has been analysed and compared with the observed data of a field campaign in 2003. Matlab codes have been developed for this purpose to manage large amount of data efficiently.

The comparisons of model and observed velocity in the estuary show that the model results fit well with the reality. Flooding and drying events in the mudflats are well represented and the magnitudes of model velocity and directions follow the natural pattern influenced by tides. Therefore, further research work in erosion and sedimentation processes can be performed based on the hydrodynamic numerical model developed in this thesis.

## **List of Tables**

Table 3-1: Geographic Data Description.....	10
Table 6-1: Performance of the model velocity magnitudes along Tide.....	49
Table 6-2: Performance of the 2-D Hydrodynamic model along the transversal sections at different tidal phases.....	52

## List of Abbreviations

ADCP	Acoustic Doppler Current Profiler
AMINAL	Administratie Milieu-, Natuur-, Land- en Waterbeheer
AWZ	Flemish Waterways and Maritime Affairs
CTD	Conductivity-Temperature-Depth
DEM	Digital Elevation Model
ED50	European Datum 1950
EDF-DRD	Research and Development Directorate of the French Electricity Board
EPA	Environmental Protection Agency (United States)
FSE	Free Surface Elevation
GOF	Goodness of Fit
IDW	Inverse Distance Weighted interpolator
LNHE	Laboratoire National d'Hydraulique et Environnement (France)
MLLWS	Mean of the Lowest Low Water at Spring Tide
RMSE	Root Mean Square Error
SWE	Shallow Water Equation
TAW	Tweede Algemene Waterpassing
TIN	Triangulated Irregular Network
UTM	Universal Transverse Mercator
WGS84	World Geodetic System 1984

## **Errata for Master Dissertation: 2D hydrodynamic modelling of a tidal inlet using TELEMAC. Case study of 'De IJzermonding'**

Page 13, line 6 from bottom

Change the sentence to **The amplitude ( $A$ ) of the wave is taken as 2.25, representing the mean of spring and neap tide.**

Page 16, Change Figure number **0-1** to **4-1**.

Page 24, line 4

Change **physical characteristics** to **geometry**.

Page 37, line 11 from bottom

Add after (closed boundary) **and a marina on the right bank**.

Page 40, line 7 from bottom

Change **25,920** to **86,400**